Phase equilibrium modelling of partial melting in the upper mantle: A comparison between different modelling methodologies and experimental results

Tahnee Otto, Gary Stevens, Matthew Jason Mayne, Jean-François Moyen

LITHOS 444-445 (2023) 107111

Contents lists available at ScienceDirect

LITHOS

journal homepage: www.elsevier.com/locate/lithos

Phase equilibrium modelling of partial melting in the upper mantle: A comparison between different modelling methodologies and experimental results

Tahnee Otto [a,*], Gary Stevens [a], Matthew Jason Mayne [a], Jean-François Moyen [b]

[a] Department of Earth Sciences, Stellenbosch University, Private Bag X1, 7602, South Africa
[b] Université de Lyon, UJM, LMV, 23 rue Dr. Paul Michelon, F-42023 Saint Etienne, France

ARTICLE INFO

Keywords:
Phase equilibrium modelling
Thermodynamic modelling tools
Experimental petrology
Partial melting
Upper mantle
SCLM

ABSTRACT

Recent advances in thermodynamic modelling now allow phase equilibrium studies of partial melting in mafic and ultramafic sources under upper mantle conditions. This potentially offers several advantages over experimental investigations, including the fact that capsule-sample interactions are avoided, there is no uncertainty over the volatile content of the charge, the process is much faster, and open system behaviour can be investigated with relative ease. Two different thermodynamic datasets are in common use for phase equilibrium investigations of mantle rocks, compiled alongside a range of constantly evolving phase solution models. This study compares the results of published experimental studies on partial melting in the upper mantle with phase equilibrium modelling results from the popular pMELTS software (Ghiorso et al., 2002), which uses an embedded dataset from Berman (1988), and with results from the Rcrust software (Mayne et al., 2016), which uses the dataset of Holland & Powell (2011). The aim of this comparative study is to investigate the suitability of each combination of software specific calculation routines, thermodynamic datasets and phase solution models to provide a viable alternative to conventional experimental techniques when studying magma genesis from the upper mantle. The main points of interest are how the phase assemblages, proportions, and compositions predicted by the modelling compare with those produced in the experiments. The set of experimental results used for comparison includes both peridotitic and eclogitic compositions, investigated over a pressure range of 1.0–3.0 GPa and a temperature range of 1165–1950 °C. The results indicate that using the Holland & Powell (2011) dataset and appropriately selected phase solution models provides the best match with experimental results in terms of melt volume, melt composition and the assemblage of coexisting phases produced during partial melting under upper mantle conditions.

1. Introduction

Understanding the mechanisms of partial melting in the upper mantle is essential to understanding energy and mass transfer between the mantle and the crust. Experimental studies have provided insight into the partial melting behaviour of a range of possible mantle source compositions that may produce mafic to intermediate magmas (e.g. Baker and Stolper, 1994; Ito and Kennedy, 1973; Kushiro, 2001 and references therein; Takahashi et al., 1993). However, as detailed in a subsequent section of the manuscript, conducting partial melting experiments at pressures and temperatures relevant to even the uppermost mantle is difficult for a variety of reasons, principally because the temperature range of interest is above the melting point of gold, a common capsule material used in experiments. Consequently, capsules consisting of platinum group elements must be used and these all alloy with iron (e.g. Brugier et al., 2015; Merrill and Wyllie, 1973), resulting in the common usage of graphite inner capsules or liners (e.g. Falloon et al., 1988; Wang et al., 2020). The result is that the effective bulk composition in such experiments may be different from the intended composition, particularly with regards to volatile content, fugacity (f) of volatile content, Fe content and Mg# (e.g. Médard et al., 2008; Merrill and Wyllie, 1973). Thermodynamic modelling does not have these problems, but does have problems with the availability of suitable experimental data on the thermodynamic properties of minerals. This

* Corresponding author.
E-mail addresses: tahneeotto@sun.ac.za (T. Otto), gs@sun.ac.za (G. Stevens), mmayne@sun.ac.za (M.J. Mayne), jean.francois.moyen@univ-st-etienne.fr (J.-F. Moyen).

https://doi.org/10.1016/j.lithos.2023.107111
Received 11 November 2022; Received in revised form 27 February 2023; Accepted 3 March 2023
Available online 10 March 2023

may result in imperfect and incomplete thermodynamic datasets and activity-composition (*a-x*) models for solid and liquid solution phases, which are thus inadequate to express the complexity of solid solution behaviour in minerals, particularly at mantle pressures where a range of pressure sensitive substitutions become important in micas, pyroxenes, and amphiboles (e.g. Holland et al., 2018).

Recently, thermodynamic modelling has been expanded to enable phase equilibrium studies of partial melting in mafic and ultramafic sources (Ghiorso et al., 2002; Holland et al., 2018; Tomlinson and Holland, 2021) under upper mantle pressure-temperature (P-T) conditions using a variety of different software (e.g. Connolly and Kerrick, 1987; de Capitani and Petrakakis, 2010; Ghiorso et al., 2002; Powell and Holland, 1988; Riel et al., 2022) that utilise at least two different thermodynamic datasets i.e. Berman (1988) and Holland and Powell (2011). Additionally, methodologies and software have also been developed to investigate open system behaviour, such as melt loss (e.g. Mayne et al., 2016; Xiang and Connolly, 2022) or magma movements (Bohrson et al., 2014). These developments have evolved phase equilibrium modelling into a useful and powerful tool for igneous rock studies, providing several crucial advantages over experimental studies, such as the ability to conduct investigations much faster with greater P-T resolution on any composition of the investigators choice (within the limits of modelling capabilities), and the ability to simulate open system processes. These techniques could be very beneficial to advancing understanding of mantle melting, if phase equilibrium approaches can be shown to be sufficiently accurate.

Underpinning all thermodynamic modelling applications are thermodynamic datasets of liquid and solid species, including databases of standard-state properties as well as sets of *a-x* models that define the variation in thermodynamic properties of liquid and solid solution phases. Table 1 provides a summary of some of the software/front-ends that are available for modelling upper mantle behaviour, and their calculation strategies. The next section of the manuscript expands on these details by discussing the available thermodynamic datasets and *a-x* models applicable to the software.

The complexity that exists with different modelling approaches, different thermodynamic datasets and different *a-x* models, as well as the uncertainties introduced by the fact that some experiments may not be "on composition" (i.e. the true effective bulk composition deviates from that reported), means that comparisons involving one set of experiments with one modelling exercise might miss crucial discrepancies and do not test how well a particular modelling platform replicates experimental data within upper mantle P-T-composition ranges. This study aims to address this by comparing the results of a range of partial melting experiments on ultramafic and mafic compositions under P-T conditions appropriate to the subcontinental lithospheric mantle (SCLM), with the results from phase equilibrium modelling conducted with multiple software packages. Additionally, thermodynamic modelling is used to produce an envelope of uncertainty around the experimental results that considers the uncertainties in Fe, H_2O and CO_2 content that are inherent to the experimental design. By comparing the outputs produced via modelling exercises utilising pMELTS (Ghiorso et al., 2002) using the embedded thermodynamic dataset from Berman (1988), and Rcrust (Mayne et al., 2016), which performs minimisation using Perple_X in the thermodynamic dataset of Holland and Powell (2011), with the results of experimental studies of selected eclogitic and peridotitic bulk compositions, extended evaluation of the performance of these modelling tools across a range of temperatures at 1.0–3.0 GPa can be performed. Comparative investigations not only contribute to the improvement of the individual tools, but also provide insights into the variation that may be observed when using different software bundles, ultimately aiding in the selection of the appropriate modelling platform when considering upper mantle P-T-X conditions for investigation. Details of how the modelling was conducted are provided in the methodology section, and the outputs are reported in Appendix A.

Table 1
Calculation strategies of some of the thermodynamic modelling software/front-ends available for conducting investigations under upper mantle conditions.

Software/front-end	Calculation strategy
THERMOCALC[1]	Solving for reaction boundaries where dG = 0
Theriak/Domino[2]	Gibbs free energy minimisation
Perple_X[3]	Gibbs free energy minimisation
Rcrust[4]	Gibbs free energy minimisation inherited from Perple_X. Path-dependant iterations allow compositional change
MELTS Family[5]	Gibbs free energy minimisation with P-T input, or minimisation of other energies

[1] Powell & Holland (1988); Powell et al. (1998).
[2] de Capitani & Brown (1987); de Capitani and Petrakakis (2010).
[3] Connolly (2005, 2009); Connolly and Kerrick (1987).
[4] Mayne et al. (2016; 2019).
[5] Asimow & Ghiorso (1998); Ghiorso and Sack (1995); Ghiorso et al. (2002).

2. Thermodynamic modelling under upper mantle conditions – the available tools

The ongoing expansion of phase equilibrium modelling as a tool to understand metamorphic and igneous processes has produced a range of different applications (Lanari and Duesterhoeft, 2019). This section does not attempt a comprehensive review of all of the available options for conducting modelling at upper mantle P-T conditions (see Riel et al., 2022; Xiang and Connolly, 2022), rather the work focusses on the differences in modelling strategies and/or the thermodynamic datasets used in some of the commonly utilised applications, so that the non-specialist reader can understand why the same phase equilibria modelling exercise may produce different results when processed through different applications.

2.1. MELTS family

MELTS is a thermodynamic software, solution model, and dataset package designed to facilitate thermodynamic modelling of phase relations during melting and crystallisation in magmatic systems (Asimow and Ghiorso, 1998; Ghiorso and Sack, 1995). The original MELTS package was primarily developed for fractional crystallisation processes in systems of basic composition (Ghiorso and Sack, 1995), having since expanded to have the widest uptake of all the thermodynamic modelling packages in the Igneous Petrology community, particularly for mantle studies. Designed principally for forward modelling of igneous processes using a constrained energy minimisation approach (Hirschmann et al., 1998a), MELTS utilises embedded thermodynamic *a-x* models of solid and liquid phases alongside energy optimisation techniques that are dependent on the process under investigation. These techniques utilise iterative application of three different algorithms: estimates of stable phase identities and compositions; minimisation of applicable thermodynamic potential(s) subject to compositional constraints, whilst other variables remain constant; and metastability examinations of resultant computed phases in relation to possible miscibility gaps or additional phases excluded in initial phase assemblages (Hirschmann et al., 1998a). For MELTS, the standard-state properties of end-member mineral components are based on the internally-consistent dataset of Berman (1988), with several exceptions detailed by Sack and Ghiorso (1994) and references therein. The mixing properties for solid solutions are drawn from several works detailed in Hirschmann et al. (1998a).

The original MELTS bundle has been superseded by several versions with modifications to allow applicability over a range of applications. This includes the rhyolite-MELTS bundles (Gualda et al., 2012), which are used to investigate crystallisation in natural composition magmas (basalts to rhyolites) below 2.0 GPa. rhyolite-MELTS is available in three versions: (i) the original version, 1.0.2., which excludes CO_2-bearing systems; (ii) version 1.1.0., suitable for silicic systems that are CO_2-

bearing (Ghiorso and Gualda, 2015); and (iii) version 1.2.0., suitable for mafic, intermediate and alkalic CO_2-bearing systems and for calculating mixed fluid saturation. Additionally, the pMELTS bundle (Ghiorso et al., 2002) is optimised for investigating anhydrous or nominally anhydrous (pHMELTS, Asimow et al., 2004) mantle bulk compositions such as peridotites and pyroxenites from 1.0 to 3.0 GPa and 1000–2500 °C.

2.2. THERMOCALC

The software THERMOCALC performs thermodynamic calculations using a non-linear equation approach to solve mineral equilibria problems (Holland and Powell, 1998; Powell et al., 1998; Powell and Holland, 1990). The THERMOCALC application utilises an internally-consistent thermodynamic dataset to construct and solve chemical potential calculations, supplemented by mass-balance or constraints on compositional variables where necessary, i.e. by solving for the points where the change in Gibbs free energy between two potential assemblages is zero, a reaction boundary is found. This allows the prediction of phase assemblages and phase compositions by utilising both forward and inverse calculation facilities, under user-specified conditions (Powell et al., 1998; Worley and Powell, 2002). THERMOCALC originated as a metamorphic petrology tool and evolved from the approach of constraining simple system grid topology as a means of understanding metamorphic reactions (Powell and Holland, 1988). The development of *a-x* models for melt (Holland and Powell, 2001) allowed the software to find substantial applicability in the study of partial melting of metamorphic rocks, and ultimately to the investigation of igneous processes (Holland et al., 2018; Jennings and Holland, 2015; Tomlinson and Holland, 2021).

The thermodynamic data underlying phase equilibria calculations in THERMOCALC is read in the form used by HP*x*-eos (White et al., 2007), which are thermodynamic solution models for geological phases, fluids, and silicate melts. The building blocks of an HP*x*-eos include a set of compositional end-members, as well as a set of *a-x* relations (Holland and Powell, 1996a, 1996b; Powell and Holland, 1993) which describe the end-member mixing thermodynamics. The most current sets of HP*x*-eos families are the Metapelite set (White et al., 2014), suitable for use below 1.5 GPa; the Metabasite set (Green et al., 2016), suitable for use below 2.0 GPa; and the Igneous set (Holland et al., 2018; Tomlinson and Holland, 2021), suitable for partial melting of basaltic to granitic melt compositions, allowing anhydrous ($\leq$ 6.0 GPa) and hydrous ($\leq$ 3.0 GPa) calculations. These HP*x*-eos families are built on the revised Holland and Powell (2011) dataset, which has undergone several updates from its previous versions (Holland and Powell, 1985, 1990, 1998).

Multiple thermodynamic modelling software have implemented the use of the HP*x*-eos families and the Holland and Powell (2011) dataset, including Perple_X (Connolly, 2005; Connolly and Kerrick, 1987) and Theriak/Domino (de Capitani and Brown, 1987; de Capitani and Petrakakis, 2010). As a result, THERMOCALC and such other programs should produce identical outputs for calculations involving the same thermodynamic dataset and *a-x* models, as has been shown to be the case (e.g. Connolly, 2007, 2021; Horváth, 2007). This application of the HP*x*-eos and Holland and Powell (2011) dataset requires regular updates across platforms, and routine benchmark comparisons provide quick insights into the correct implementation of such input data to other programs.

2.3. Theriak/Domino

Theriak/Domino is a software program collection that uses a linear programming strategy combined with a Gibbs free energy minimisation calculation method to conduct and produce a wide range of thermodynamic equilibrium calculations and illustrations, including thermodynamic functions of phases, phase diagrams, equilibrium assemblages, and pseudosections (de Capitani and Brown, 1987; de Capitani and Petrakakis, 2010). The equilibrium phase compositions and stable mineral assemblage for a bulk rock composition along a specified P-T path or set of P-T conditions is calculated using the Theriak program, and Domino is used for plotting a range of equilibrium assemblage diagrams (de Capitani and Petrakakis, 2010). Theriak/Domino has compatibility with the currently available thermodynamic datasets, and the capability of porting most THERMOCALC HP*x*-eos families, as mentioned above. An add-on to the Theriak/Domino software package, Theriak_D works as an interface to process thermodynamic data in a programming environment outside the Theriak/Domino package (Duesterhoeft and de Capitani, 2013).

2.4. Perple_X and derivatives of the program

The software package Perple_X is a modular collection of subprograms created for the rapid computation of all types of phase diagrams, as well as performing general thermodynamic calculations (Connolly, 2005; Connolly and Kerrick, 1987). By utilising a calculation method based on minimisation of total Gibbs free energy of multiple phase configurations and pseudocompounds, Perple_X programs are able to calculate the most stable set of phase equilibria for an arbitrary chosen system (Connolly, 2005; Connolly and Petrini, 2002). The thermodynamic datasets and *a-x* models implemented in Perple_X can be selected from several compiled databases, as the software accepts thermodynamic data that has been suitably formatted for Perple_X from any source; as mentioned, the THERMOCALC HP*x*-eos families and Holland and Powell (2011) dataset are readily incorporated into Perple_X.

2.4.1. Rcrust

Rcrust is a phase equilibria modelling tool that utilises the Meemum function of Perple_X (Connolly, 2009) to calculate phase stabilities for a series of points, inheriting databases and *a-x* models from Perple_X (Mayne et al., 2016). The Rcrust calculation strategy applies path dependencies to allow bulk compositional change via processes of mass transfer. Importantly, Rcrust strategies allow the investigation of processes dependent on assemblages evolving throughout a given P-T-X space, as changes in bulk compositions are transferred across points. Prior to passing the information along, phases can be extracted or added depending on a broad range of flexible trigger signals (e.g. mode of melt, melt viscosity, phase proportion, phase to melt ratio, etc), allowing open or closed systems. Mayne et al. (2019) describe the division of the full system (bulk rock composition) into a reactive subsystem and an extract subsystem, the former being the system on which phase equilibrium modelling is conducted and the latter representing the phases that have been removed from the residual system by phase extraction events. The development of Rcrust was primarily as a tool for the forward modelling of partial melting and magma generation in the crust, but the use of Perple_X formatted input data allows Rcrust to perform modelling across any P-T-X range that is compatible with the available thermodynamic datasets and *a-x* models (Mayne et al., 2019). Thus, if the P-T resolution in Rcrust is set to match the highest resolution attained by Perple_X gridded-minimisation, Rcrust and Perple_X modelled outputs will be identical if the same *a-x* models are utilised.

2.5. Experiments compared with thermodynamic modelling

Several recent studies have compared the results of experiments with the results of thermodynamic modelling of the same bulk composition for upper mantle conditions (e.g. García-Arias, 2020; Gervais and Trapy, 2021; Ghiorso et al., 2002; Hernández-Uribe et al., 2022; Hirschmann et al., 1998a; Holland et al., 2018; Jennings and Holland, 2015; Tomlinson and Holland, 2021; Tropper and Hauzenberger, 2015). In general, most studies have concluded that modelling compares favourably with experiments, but consistent issues within the different platforms are worth noting. Hirschmann et al. (1998a) have reported a systematic difference between the melt compositions predicted by MELTS relative

to those of experiments investigating the partial melting of peridotite, with concentrations of SiO_2 initially underpredicted by 4–5 wt%. This is also reflected by MELTS predicting systematically lower melt fractions relative to experimental observations, equivalent to an approximate 100 °C offset (Hirschmann et al., 1998a). This has been improved with revisions to the pMELTS algorithm, such that the consistent underestimate in melt proportion is lower, equating to a temperature offset averaging 50 °C, and overpredictions of melt SiO_2 values are reported as lowered to approximately 1% (Ghiorso et al., 2002). Additionally, improvement in calculated liquid MgO concentrations are also reported, although still between 1 and 4% higher, and attributed by Ghiorso et al. (2002) to the temperature offset. Other known problems of pMELTS predictions include, at low pressures, the addition of Cr-spinel to the assemblage that is not observed experimentally and the continued overstabilisation of clinopyroxene relative to melt, as well as the oversaturation of garnet with increasing pressure (Ghiorso et al., 2002).

Comparisons of melt fraction curves for partial melting of peridotite from THERMOCALC with experimental results generally display good agreement near the solidus (considering a range of different experimental results), but also display systematically underestimated melt fraction at high temperatures (~20 vol%), which equates with a temperature offset of approximately 50 °C (Jennings and Holland, 2015). Consequently, the melt compositions differ significantly from experiments at higher melt fractions, especially at higher pressure. The persistence of garnet (with underestimated Cr-content) and a small fraction of spinel with melt to higher temperatures was also noted (Jennings and Holland, 2015). Revisions by Holland et al. (2018) show improvement of the melt phase liquidus temperatures, as well as improved fitting of garnet compositions with P-T change and a new *a-x* model for spinel that eliminates its default appearance up to liquidus temperatures. Overestimations of orthopyroxene abundance was noted in the Holland et al. (2018) model, and subsequently expanded upon by Tomlinson and Holland (2021) through changes made to the structure of the melt model. Another known problem of the Igneous HP*x*-eos of THERMOCALC was the stability of a high-Ca orthopyroxene phase in various rock assemblages (Green, 2020). This has reportedly been eliminated from the orthopyroxene solution model in the *x*-eos bundle from 31-10-2020 (Green, 2022), and implementations of these changes to the Perple_X formatted phase solution models was confirmed as of 02-12-2020 (Connolly, 2022).

Regardless of the issues discussed above, the results of experiments and phase equilibrium modelling results cannot be expected to correlate perfectly. Each approach has its own advantages and pitfalls, and investigations utilising one or the other cannot be classified as more or less appropriate unless these inherent aspects are considered (White et al., 2011). The more serious pitfalls of both approaches, as relevant to studies of partial melting of mantle lithologies, are briefly considered below.

At P-T conditions above the melting point of gold, the required use of Pt or AgPd capsules in experimental studies introduces potential uncertainties in the degree to which the effective bulk composition matches the intended composition, and the degree to which the fluid state of experiments is known. Although experimental studies can handle the full chemical complexity of natural rocks, the uptake of Fe by Pt or Pd capsules is known to potentially change the bulk composition (Brugier et al., 2015 and references therein; Merrill and Wyllie, 1973). Pre-saturation of the capsule alloy with Fe and the use of graphite inner capsules (liners) are common strategies to counter this (e.g. Falloon et al., 1988; Grove, 1981; Wang et al., 2020). However, the common use of graphite liners comes with its own set of problems, as it is probably impossible in most laboratories to conduct a partial melting experiment without the inclusion of some unintended O_2 or H_2O into the capsule (Médard et al., 2008). This will result in reactions between H_2O, O_2, and C (in the liner) and may result in partial melting initially occurring in a fluid-saturated system. Whilst at very low melt fractions this may be undetectable, the resultant higher fH_2O and fCO_2 must affect melting behaviour even after the system has become fluid-absent. In addition, irrespective of the fO_2 conditions of starting material synthesis, experiments conducted with graphite liners are inevitably buffered to C-CO. Thus, capsule uptake of Fe and the existence of small amounts of unintended H_2O and CO_2 in experimental charges are a potential source of discrepancy between experimental results and modelling studies that are not often considered when the outputs of modelling studies are benchmarked against experiments. In this study, phase equilibrium modelling is used to attempt to constrain the envelope of uncertainty that these factors introduce into experimental results.

In contrast, for the various designs of piston-cylinder apparatus that form the mainstay of experimental studies under upper mantle P-T conditions, measurement and control of pressure and temperature represent a potential but largely insignificant source of error. It is possible to place the thermocouple within 0.5 mm of the capsule and to control temperature to ±1 °C. Capsules of large enough volume to contain graphite liners may experience temperature gradients, however when these are tested using multiple thermocouple arrangements these are found to be low (5–10 °C across 0.8–1.0 cm capsules) (e.g. Baker and Stolper, 1994; Schilling and Wunder, 2004). Given the fact that pressure is generated hydraulically and transmitted to the capsule using a salt medium with negligible frictional losses if using the hot piston-out technique, the accuracy of the pressure gauge determines pressure uncertainty. For labs with a precision test gauge this is typically 0.1% of the measured value.

Additional experimental uncertainties revolve around the analysis of phase compositions, especially silicate glasses (quenched melts). Due to the need for a high degree of spatial resolution, the standard technique for analysing the major element compositions of phases in experimental run products is electron beam analysis, using EDS and/or WDS on an electron microprobe or scanning electron microscope. Regardless of the instrument details, the accelerating voltage (or beam energy) utilised during the analysis of silicate glass has a significant effect on the reported compositions, especially for glasses that are hydrous or have higher alkali contents (Humphreys et al., 2006; Morgan and London, 1996; Varshneya et al., 1966). In these cases, even the lowest energy beams that are viable will record a decrease in Na counts as a function of time under the beam. This is due to the migration of Na away from the analysis point, and this effect is exacerbated by the increased count-rate for immobile components such as Si and Al, increasing their relative contributions (Morgan and London, 1996). Studies try to counter this problem by using defocused beams, but freezing the sample to approximate liquid nitrogen temperatures using a cryo-stage is the only truly effective way to counter the problem (Humphreys et al., 2006; Stevens et al., 1997), which is uncommon in experimental studies.

Moreover, some glasses with mafic and ultramafic compositions are hard to identify at low melt fractions due to extensive crystallisation upon quenching (Baker and Stolper, 1994; Cawthorn et al., 1973). The methods used to increase the efficacy of the analyses, such as diamond aggregates (Baker and Stolper, 1994; Falloon et al., 1999) or carbon spheres (Wasylenki et al., 1996), have their own pitfalls that need to be considered (Falloon et al., 1996; Wasylenki et al., 2003). For example, the pressures in the void spaces of diamond aggregates are initially low, possibly leading to the separation of liquids that are not in equilibrium with the system (Wasylenki et al., 2003). Comparatively, the use of carbon spheres segregate melt due to surface effects, and requires longer equilibrations runs (increasing Fe loss to the capsule; Pertermann and Hirschmann, 2003a). Both methods will likely result in some C-bearing gas species in the charge prior to melting.

In thermodynamic modelling, bulk compositions and fluid states are set, and analytical errors sensu stricto are non-existent. Nevertheless, the internal consistency of thermodynamic datasets are important in their perceived accuracy; internal consistency is dependent on the thermodynamic properties of pure phases and end-members in thermodynamic datasets, and their interactions with *a-x* models (Lanari and Duesterhoeft, 2019). These thermodynamic properties, together with the

formulation of *a-x* models, can be a great source of systematic uncertainties (Berman, 1988; García-Arias, 2020; Holland and Powell, 2011; Powell, 1985; White et al., 2014). For example, the complexity of certain chemical components, such MnO, NiO, and P_2O_5, currently inhibit the development of complete *a-x* models to describe the activity relations of mineral phases that incorporate these components (Gervais and Trapy, 2021). The omission of these components from thermodynamic datasets is likely to be an important source of error when modelling rock compositions where these components are important to the stability of one or more phases (e.g. Forshaw et al., 2019; García-Arias, 2020). Consequently, an important consideration of thermodynamic modelling is that these calculations are wholly dependent on the input thermodynamic data, and the outcomes remain a simplification of nature — even with extended chemical systems — only reporting approximations of phase behaviours that also do not consider any kinetics, such as crystal sizes, crystal growth and nucleation, and diffusion, amongst others (García-Arias, 2020; White et al., 2011).

3. Methodology

Three sets of partial melting experiments (Table 2) were chosen for comparison with the thermodynamic modelling outcomes by means of phase assemblages, phase proportions, phase compositions, and phase-in/phase-out boundaries. The chosen studies represent compositions that include two peridotites and an eclogite: Experiments KLB-1 from the studies of Takahashi (1986) and Takahashi et al. (1993) and MM3 from Baker and Stolper (1994) and Hirschmann et al. (1998b) represent a fertile spinel lherzolite sourced from the Kilborne Hole crater, New Mexico; experiments G2 from the studies of Pertermann and Hirschmann (2003a, 2003b) represent an eclogite prepared from natural garnet and clinopyroxene sourced from the Münchberg Massif, Bavaria. Experiments KLB-1 consisted of 95 runs conducted from 1 atm to 14.0 GPa, however only the runs from 1.0 to 3.0 GPa are investigated in this study. Experiments MM3 consisted of 21 runs conducted at 1.0 GPa from 1250 °C to 1390 °C, and only the experiments where phase proportions are reported were considered. Experiments G2 consisted of six runs from 1165 to 1375 °C at 2.0 GPa, one run at 1325 °C and 2.5 GPa, and 20 runs from 1300 to 1525 °C at 3.0 GPa. Compositions of olivine, clinopyroxene, orthopyroxene, garnet, plagioclase, spinel, and glass/melt have been considered for the comparison. Where applicable, the reported experimental bulk compositions were modified to be NiO, P_2O_5, and MnO free due to an incomplete set of *a-x* models defining the compositional space.

The experimental studies have some limitations for the purpose of this study. For KLB-1, Takahashi et al. (1993) only report selected melt fractions at 1.5 GPa, and Takahashi (1986) only reports phase compositions at the P-T points of 1325 °C and 1.0 GPa, and 1550 °C and 3.0 GPa. For MM3, Baker and Stolper (1994) report phase compositions for all runs where proportions are noted, apart from 1310 °C where only the liquid composition is reported. Hirschmann et al. (1998b) provide reanalysed compositions for some of the MM3 experiments, but report only the liquid compositions at 1250 °C and 1260 °C and no additional data. The experimental works on G2 report phase proportions (Pertermann and Hirschmann, 2003a) for the majority of the investigated P-T points, except at 2.0 GPa for experiments at 1165 °C, 1185 °C, and 1225 °C. Consequently, comparisons between experimental results and thermodynamic modelling outputs were made where the relevant data was available. Additionally, where no phase proportions were reported, a sum of squared residuals mixing routine was used to calculate phase proportions from the compositional data where possible, and also to assess the soundness of reported proportions, where these were provided; these results are reported in Appendix A.

All of the studied experimental works make use of Pt-capsules with graphite liners to minimise the uptake of Fe to the capsule, and as the experiments are intended to be volatile free, the authors describe several strategies to avoid the absorption of H_2O by materials in the capsules. All three studies describe drying loaded but unsealed capsules (at 110 °C and 300 °C) for various timeframes before welding. Additionally, Baker and Stolper (1994) report including a layer of diamond powder in the capsules as a melt trap, similarly applied using carbon spheres for near solidus runs by Pertermann and Hirschmann (2003a, 2003b). Pertermann and Hirschmann (2003a, 2003b) also report packing capsules in a layer of Fe_2O_3 powder to reduce the influx of hydrogen to the experiments, a potential source of H_2O in the capsules.

In all of the studies, capsules were loaded and welded in an air environment, and therefore the development of CO_2 and CO from the reaction of air with the graphite liner is inevitable. Both H_2O and CO_2 lower the mafic and ultramafic rock solidi at upper mantle pressures. As

Table 2
Details of the experimental sets investigated in this study. Modified analyses were normalised to be NiO, P_2O_5, and MnO free. All comparisons were based on FeO_t values. (–) indicates no data available.

Experimental set	KLB-1[1]		MM3[2]		G2[3]	
Composition (wt%)	Reported	Modified	Reported	Modified	Reported	Modified
SiO_2	44.48	44.65	45.50	45.67	50.05	50.13
TiO_2	0.16	0.16	0.11	0.11	1.97	1.97
Al_2O_3	3.59	3.60	3.98	3.99	15.76	15.79
Cr_2O_3	0.31	0.31	0.68	0.68	–	0.00
FeO_t	8.10	8.13	7.18	7.21	9.35	9.36
MnO	0.12	0.00	0.13	0.00	0.19	0.00
MgO	39.22	39.37	38.30	38.44	7.90	7.91
CaO	3.44	3.45	3.57	3.58	11.74	11.76
Na_2O	0.30	0.30	0.31	0.31	3.04	3.04
K_2O	0.02	0.02	–	0.00	0.03	0.03
P_2O_5	0.03	0.00	–	0.00	–	0.00
NiO	0.25	0.00	0.23	0.00	–	0.00
Sum	100.02	100.00	99.99	100.00	100.03	100.00
Pressure (GPa)	1.5–3.0		1.0		2.0–3.0	
Temperature (°C)	1325–1950		1270–1390		1165–1525	
Reported H_2O Content	Anhydrous		Anhydrous		Nominally anhydrous	
Reported fO_2	NNO		Below GCO (C-CO) buffer		Below C-CO buffer	
Reported Capsule Material	Graphite-lined/Re foil lined Pt-Capsules		Graphite-lined Pt-Capsules		Graphite-lined Pt-Capsules	

[1] Fertile spinel lherzolite from Takahashi (1986) and Takahashi et al. (1993).
[2] Fertile spinel lherzolite from Baker and Stolper (1994) and Hirschmann et al. (1998b).
[3] Bi-mineralic eclogite from Pertermann and Hirschmann (2003a, 2003b).

a result, thermodynamic modelling was used to investigate the uncertainty that may accompany experimental results if small but realistic amounts H_2O or CO_2 were unintentionally included in the capsule. Similarly, the effects of the loss of Fe to the capsule were also investigated, the details of which are described below.

The thermodynamic modelling software utilised in the comparative study investigating closed system evolution includes pMELTS (mafic and ultramafic compositions) and Rcrust (ultramafic to intermediate compositions). The outcomes for all comparisons have been recorded in Appendix A. Firstly, runs were performed for each P-T point listed in the relevant experiments using the latest pMELTS (version 5.6.1.) bundle in the NKCFMASTOCr (Na_2O-K_2O-CaO-FeO-MgO-Al_2O_3-SiO_2-TiO_2-Fe_2O_3-Cr_2O_3) chemical system, embedded with the thermodynamic dataset from Berman (1988) with modifications detailed in Ghiorso et al. (2002), and *a-x* models included in the pMELTS calibration. The system was considered H_2O and CO_2 free, and the fO_2 was set along the C-COH buffer for the three source compositions. Phase assemblages, phase proportions, and phase compositions were recorded at the specific P-T conditions of each experiment performed in the experimental set within the range of 1.0 to 3.0 GPa. As pMELTS outputs FeO and Fe_2O_3, direct comparison to experimental results required recalculation to FeO_t.

Secondly, runs were performed for each P-T point listed in the relevant experiments in the NKCFMASTOCr chemical system using Rcrust version 2022-09-03, the 2022 revised hp634ver.dat thermodynamic data file from Perple_X, and the internally consistent dataset of Holland and Powell (2011). The following *a-x* models were used: Cpx (TH) for clinopyroxene, Gt(TH) for garnet, Opx(TH) for orthopyroxene, Sp(TH) for spinel, and melt(TH) for melt (Tomlinson and Holland, 2021), O(HGP) for olivine (Holland et al., 2018), Fsp(C1) for plagioclase and potassium-feldspar (Holland and Powell, 2003), and Ilm(WPH) for ilmenite (White et al., 2000). Adjustments made to *a-x* model parameters are listed in Appendix A. Similar volatile content and fO_2 constraints were applied as is described for the pMELTS bundle; data was also recorded similarly.

Thirdly, the effects of Fe loss, and H_2O or CO_2 addition was modelled similarly to that described above, with changes made to the reported bulk compositions of KLB-1 and MM3 assuming either a 10% decrease in the FeO_t content, or the inclusion of 0.05 wt% H_2O, or 0.08 wt% CO_2 in the capsule. These are upper realistic boundaries for water adsorbed to the charge and liner and CO_2 production by air included the capsule. Runs were performed using Rcrust in a similar manner as above, but using the 2020 revised hp633ver.dat thermodynamic data file from Perple_X, and the following *a-x* models: Cpx(HGP) for clinopyroxene, Gt (HGP) for garnet, O(HGP) for olivine, Opx(HGP) for orthopyroxene, and Sp(HGP) for spinel (Holland et al., 2018), melt(HGPH) for melt (Heinrich and Connolly, 2022; Holland et al., 2018), Fsp(C1) for plagioclase and potassium-feldspar (Holland and Powell, 2003), and Ilm(WPH) for ilmenite (White et al., 2000). The use of this set of *a-x* models is due to the ability of the selected melt model to accommodate H_2O and CO_2. The adapted bulk compositions and results are reported in Appendix A.

Quantification of the differences between experimental results and modelling outputs for the reported experimental and modelled phase assemblages was achieved using the model quality factor Q*asm* (Lanari and Duesterhoeft, 2019), expressed as:

$$Q_{asm} = \frac{l}{k} \times 100 \quad (1)$$

where l is the number of matching phases between experimental results and modelled outputs and k is total number of phases present. Q*asm* is reported for each relevant P-T point listed in the experimental sets, and bulkQ*asm* is reported for all conditions combined. Percentage difference and relative difference was calculated where the relevant data was available in order to evaluate the match of predicted and experimental phase compositions. Percentage difference was calculated for each component in a phase as:

$$\%Difference = \frac{(m-e) \times 100}{e} \quad (2)$$

where m is the modelled value and e is the experimental value (García-Arias, 2020). This quantification was also used for phase proportions. Relative difference (or sum of residuals^2) was used to evaluate the goodness of fit between modelled and experimental compositions, calculated for each component in the phase as:

$$Sum\ of\ residuals^2 = \varepsilon(m-e)^2 \quad (3)$$

Relative differences of ≤ 4 (2^2 wt% difference) suggests a good fit, ≥ 25 (5^2 wt% difference) suggests a bad fit, and values of 4–25 suggest a reasonable fit.

4. Results

4.1. Comparison of relevant experimental results with thermodynamic modelling

The full set of thermodynamic modelling results from KLB-1, MM3, and G2 are reported in Appendix A.

4.1.1. KLB-1: partial melting of peridotite under upper mantle conditions

Both the experiments and modelling agree in the presence of olivine, orthopyroxene, clinopyroxene, garnet, spinel and melt, with very similar Q*asms* displayed for Rcrust and pMELTS, as shown in Table 3. The phase assemblages from the experiments and modelled outcomes by pMELTS and Rcrust in this study at 1.5 and 3.0 GPa are illustrated in Fig. 1, and comparisons between melt fraction (in wt%) as a function of temperature at 1.5 and 3.0 GPa is illustrated in Fig. 2.

For the majority of the pressure range investigated, pMELTS predicts the position of the solidus at lower temperatures than the experiments, similarly at 1.0 and 1.5 GPa by Rcrust (Fig. 1). In terms of the liquidus, the experimental study and Rcrust show reasonable agreement at 1.5 and 3.0 GPa, although the exhaustion of olivine is 50 °C lower at higher pressure (Fig. 1). In comparison, pMELTS predicts the liquidus to be at considerably lower temperatures at both low and high pressures, with the exhaustion of olivine predicted 200 °C lower at 1.5 GPa due to a rapid increase in the melt fraction (Figs. 1 & 2). As displayed in Fig. 1, the spinel phase predicted by both modelling bundles persists to higher temperatures than observed in the experimental assemblages, but show good agreement with experiments at 1.0 GPa (Appendix A). At low and high pressures, pMELTS predict the presence of pyroxenes at higher temperatures than the experimental data, similarly by Rcrust at low pressure. At 3.0 GPa, the garnet phase predicted by Rcrust is exhausted at 50 °C lower, whilst pMELTS delays garnet exhaustion by 50 °C.

In terms of phase compositions (Table 3 & Appendix A), modelled

Table 3
Scoring of the modelled assemblages (bulk Q*asm*) and compositions (sum of residuals^2) from pMELTS and Rcrust in comparison with the experimental study on KLB-1 of Takahashi (1986) and Takahashi et al. (1993), where such data was available.

Assemblage: Q*asm*				
Bulk Q*asm* in 33 experiments		Rcrust 78.05		pMELTS 74.24
Compositions: Sum of residuals^2				
	1.0 GPa, 1325 °C		3.0 GPa, 1550 °C	
	Rcrust	pMELTS	Rcrust	pMELTS
Ol	0.47	0.01	3.35	6.32
Opx	11.26	3.52	1.10	9.14
Cpx	28.19	15.13	4.21	27.61
Sp	616.94	12.79	–	–
Gt	–	–	–	21.94
Melt	108.74	7.92	51.00	173.97

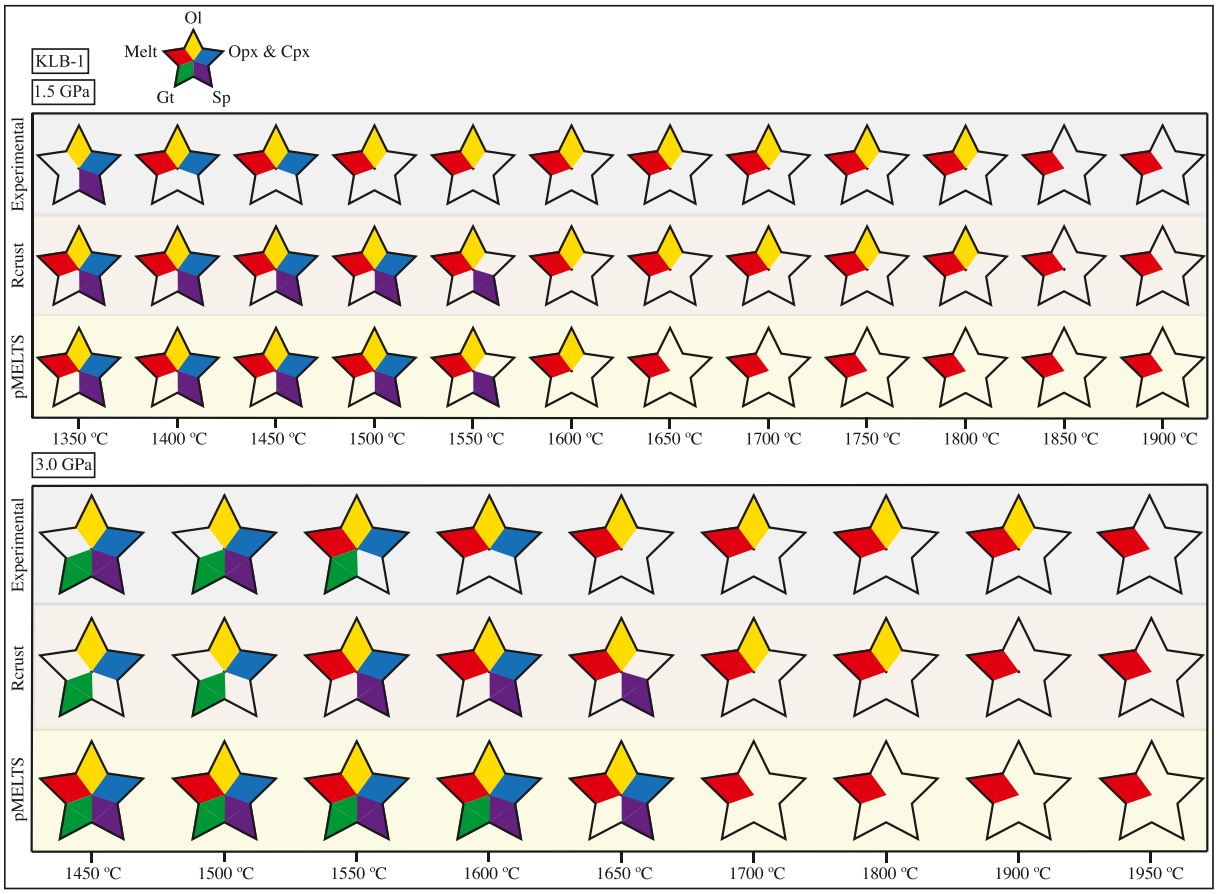

Fig. 1. A comparison of the phase assemblages from the experimental study of Takahashi (1986) on composition KLB-1 with the modelled assemblages produced using pMELTS and Rcrust in this study. The results are at 1.5 and 3.0 GPa for the temperature values indicated. Note that at 1.5 GPa, both modelling outputs predict the solidus at lower temperatures, however, Rcrust and the experimental study are in good agreement for the position of the liquidus, whereas pMELTS predicts the liquidus at a much lower temperature. At 3.0 GPa, Rcrust and the experimental study are in good agreement for the position of both the solidus and liquidus, whilst pMELTS predicts both to be at considerably lower temperatures. Rcrust does not predict spinel below 1550 °C at 3.0 GPa, and both sets of modelling outcomes predict spinel exhaustion at much higher temperatures at both pressures.

melts shows bad agreement with experiments at 3.0 GPa. A great mismatch is displayed by pMELTS due to overestimated FeO (+94.91%), MgO (+28.10%), and Na_2O (+180.45%), and underestimated SiO_2 (−14.37%), Al_2O_3 (−35.33%), and CaO (−39.47%). However, the melts predicted by pMELTS at 1.0 GPa show reasonable agreement with experiments. At high and low pressures, Rcrust predicts lower Al_2O_3 (−30.06% & −22.44%) and higher MgO (+89% & +30.40%) in the melt, and lower CaO (−25.25%) at 3.0 GPa. For the mineral phases, pMELTS and Rcrust are both in good agreement with the experimental data for the olivine composition at low pressure, but pMELTS shows only reasonable agreement at 3.0 GPa due to FeO values (+28.33%). For orthopyroxene, both modelling bundles show good to reasonable agreement with experiments, but bad agreement for clinopyroxene is observed for Rcrust (+29.63% CaO & −37.46% Al_2O_3) and pMELTS (+47.16% CaO & −8.51% MgO) at 1.0 and 3.0 GPa, respectively. At high pressure, pMELTS shows reasonable agreement with experimental garnet compositions, apart from MgO (−11.96%), whilst Rcrust does not predict garnet above 1500 °C. The spinel composition of pMELTS matches experimental results reasonably, apart from Cr_2O_3 (+16.57%) and Al_2O_3 values (−21.75%), with Rcrust displaying a bad match due to Al_2O_3 (−29.83%), MgO (−12.41%), and Cr_2O_3 (+133.29%).

4.1.2. *MM3: partial melting of peridotite under upper mantle conditions*

Comparison of the MM3 experiments with the results from pMELTS have previously been conducted by Ghiorso et al. (2002), however, the comparison has been repeated here to analyse predicted peridotite partial melting behaviour in Rcrust at 1.0 GPa using a more detailed experimental dataset. In this study, both the experiments and modelling agree in the presence of olivine, orthopyroxene, clinopyroxene, spinel and melt, with Rcrust predicting 100% and pMELTS almost 95% of the assemblage, as is reported in Table 4. Comparisons between abundances of melt, clinopyroxene, orthopyroxene, olivine and spinel as a function of temperature at 1.0 GPa are illustrated in Fig. 3. Fig. 4 displays components from the experimental and modelled melt compositions as a function of increasing melt fraction (in wt%) and increasing temperature.

Both pMELTS and Rcrust are in good agreement with experimental phase abundances (Fig. 3), however, lower modelled melt fractions can be observed for pMELTS, and for Rcrust below 1310 °C. Rcrust has an overall smaller percentage difference between experimental and Rcrust predicted melt abundances (14–42% versus 17–83% in pMELTS). Most Rcrust and pMELTS predicted melt compositions (Appendix A, Table 4) show bad agreement with experimental results, yet pMELTS predicts the only good match at 1390 °C.

When considering the composition of the melts (Fig. 4), pMELTS predicted values as a function of melt fraction match well with experimental values for SiO_2 (at higher fractions), FeO, CaO and Na_2O, but under-and overpredicts Al_2O_3 values and overpredicts MgO. The proposed ~1% overestimate in melt SiO_2 reported by Ghiorso et al. (2002) is found to be ~2% for the majority of the melting range in this study. For Rcrust, FeO, CaO and Na_2O matches well with the experimental melts, whereas underpredictions of SiO_2, Al_2O_3 and MgO are observed.

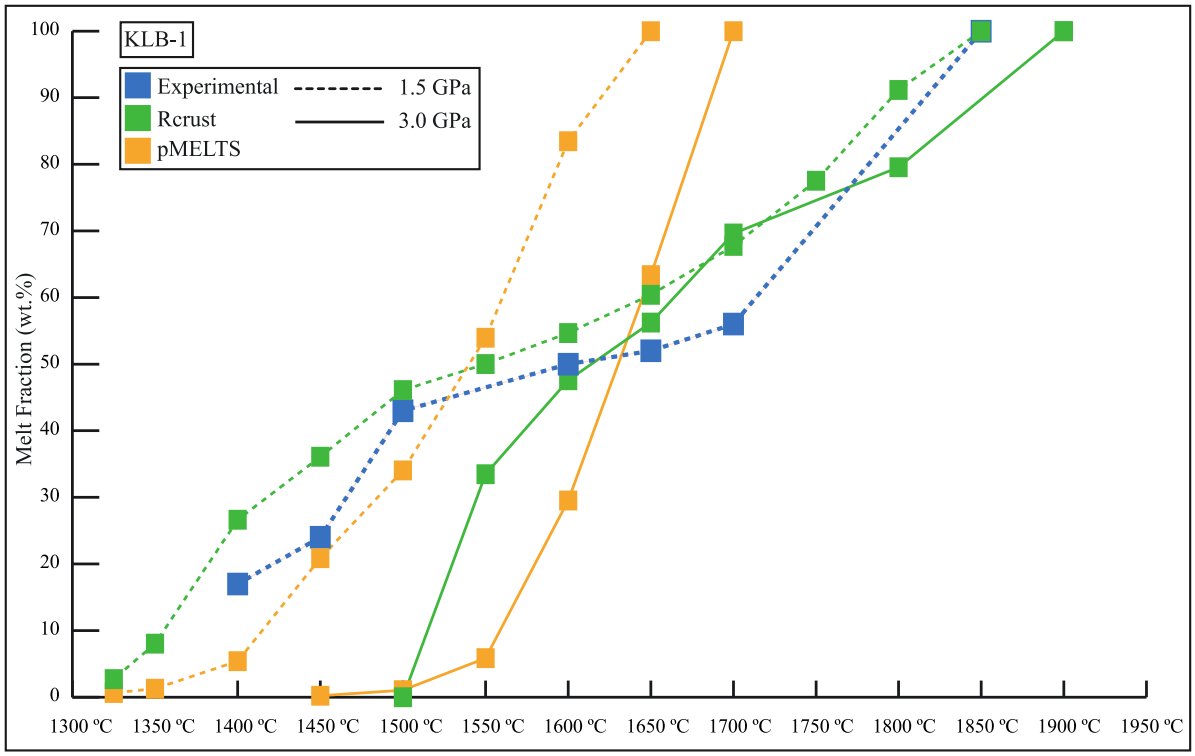

Fig. 2. Modelled melt fractions at 1.5 GPa and 3.0 GPa from pMELTS and Rcrust as determined in this study, compared with melt fractions from the experimental study on KLB-1 of Takahashi et al. (1993) at 1.5 GPa (the only pressure that phase proportion information was reported in the experimental study within the pressure range of 1.0 to 3.0 GPa). At 1.5 GPa, pMELTS predicts the liquidus to be at much lower temperatures than the experiments, whereas there is excellent agreement between melt fraction (and consequently, olivine consumption) predicted by Rcrust and the experiments. A similar melt-curve is displayed by pMELTS at 3.0 GPa, which is not the case for Rcrust.

Table 4
Scoring of the modelled assemblages (bulk Q*asm*) and compositions (sum of residuals^2) from pMELTS and Rcrust in comparison with the experimental study on MM3 of Baker and Stolper (1994) and Hirschmann et al. (1998b), where such data was available.

Assemblage: Q*asm*										
			Rcrust				pMELTS			
Bulk Q*asm* in 8 experiments			100.00				94.87			
			Compositions: Sum of residuals^2							
1.0 GPa	1250 °C		1260 °C		1270 °C		1280 °C		1300 °C	
	Rcrust	pMELTS	Rcrust	pMELTS	Rcrust	pMELTS	Rcrust	pMELTS	Rcrust	pMELTS
Ol	–	–	–	–	0.48	0.55	0.06	0.07	0.83	0.96
Opx	–	–	–	–	7.23	6.44	9.48	3.86	7.38	4.96
Cpx	–	–	–	–	1.62	3.96	1.17	4.27	2.78	4.72
Sp	–	–	–	–	70.14	102.21	20.25	58.59	104.73	298.66
Melt	96.91	15.88	38.12	43.16	28.73	72.81	26.13	68.90	28.51	54.57
1.0 GPa	1310 °C		1330 °C		1350 °C		1360 °C		1390 °C	
	Rcrust	pMELTS	Rcrust	pMELTS	Rcrust	pMELTS	Rcrust	pMELTS	Rcrust	pMELTS
Ol	–	–	0.60	0.91	0.94	1.27	0.82	1.10	1.33	1.59
Opx	–	–	9.48	2.96	7.50	2.71	5.25	3.62	4.56	5.56
Cpx	–	–	8.16	6.13	–	–	–	–	–	–
Sp	–	–	134.46	764.42	105.02	845.91	76.25	284.60	22.11	151.53
Melt	39.91	34.84	37.54	22.13	48.10	13.12	10.22	39.27	58.87	4.15

When considering the same components of melt with increasing temperature, the pMELTS values show pronounced differences from experimental data, particularly at lower melt fractions. Rcrust shows better overall agreement, but discrepancies are also obvious. For olivine, the modelled compositions (Appendix A) match well with experiments across the entire temperature range (Fig. 3 & Table 4). Although clinopyroxene proportions are higher in modelled results, good to reasonable agreement can be seen in terms of its composition. Experimental orthopyroxene has mostly good matches with pMELTS proportions and compositions across the entire temperature range, and Rcrust values generally agree reasonably with experiments. Although Rcrust and pMELTS shows good agreement in terms of spinel stability and proportions, the modelled compositions generally agree badly with experiments, except for Rcrust predictions at 1280 °C and 1390 °C.

4.1.3. G2: partial melting of eclogite under upper mantle conditions

Both the experiments and modelling agree in the presence of clinopyroxene, garnet, rutile, quartz, plagioclase and melt, with a higher Q*asm* for Rcrust as is reported in Table 5. Due to the limited phase proportion data reported in the experimental study at 2.0 GPa and only a

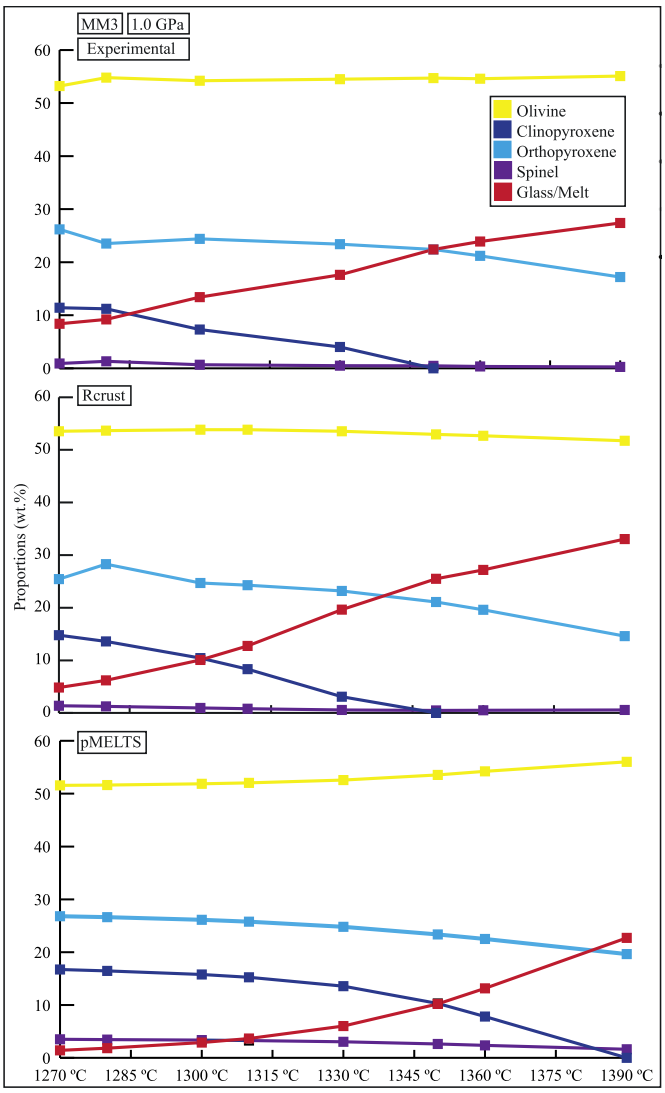

Fig. 3. A comparison of melt (glass), olivine, clinopyroxene, orthopyroxene and spinel abundances at 1.0 GPa from the experimental study on MM3 of Baker and Stolper (1994) and Hirschmann et al. (1998b), with the calculated values from pMELTS and Rcrust as determined by this study. Compared to experiments, both Rcrust and pMELTS predict lower melt abundances at 1270 °C, and the rate of increase in melt fraction predicted by pMELTS is slower than the experiments and Rcrust, displayed by the subsequent slower consumption of clinopyroxene. Rcrust and pMELTS outputs for olivine vary as temperature increases, showing overestimations of olivine abundance by pMELTS, and underestimations by Rcrust. Both modelling bundles predict very similar orthopyroxene abundances and rates of orthopyroxene consumption.

single run at 2.5 GPa, Fig. 5 displays comparisons between phase abundances as a function of temperature at 3.0 GPa only. Fig. 6 displays components from the experimental and modelled melt compositions as a function of increasing melt fraction (in wt%) and increasing temperature.

In Fig. 5, the appearance of rutile and quartz in the Rcrust modelled assemblage match the experimental results, although slightly greater in proportion; pMELTS does not predict rutile or quartz as part of the assemblage. Although both bundles predict larger abundances of garnet, its exhaustion occurs at the same temperature in the experiments and Rcrust, whereas for pMELTS, it fluctuates consistently around an approximate 32–35 wt% across the P-T range considered, and its exhaustion will thus occur at significantly higher temperatures. In Rcrust calculations, clinopyroxene disappears at a lower temperature than in the experiments, with the opposite observed for pMELTS. Rcrust predicts a slightly faster increase in melt fraction, whereas pMELTS predicts the liquidus to be at much higher temperatures, resulting in a much slower increase in the melt fraction and consequently delaying the exhaustion of garnet and clinopyroxene (Fig. 6).

Considering phase compositions (Table 5 & Appendix A), at 2.0 GPa, the Rcrust melt compositions show good agreement with experiments, except for the bad fit of the melt composition at 1250 °C. pMELTS displays a bad fit with the experimental melts at all temperatures at 2.0 GPa. Experimental and Rcrust plagioclase compositions at 1250 °C agree badly, with mismatches for Al_2O_3 (+27.85%) and CaO (+27.04%); pMELTS does not predict any plagioclase here. At 2.5–3.0 GPa, compositional comparisons could be made for clinopyroxene, garnet, and melt, except for the 1300 °C run at 3.0 GPa, where no melt was detected in the experiments or Rcrust calculations. Clinopyroxene and garnet compositions predicted by pMELTS show reasonable agreement with experiments, whereas Rcrust displays bad to good agreement with experimental clinopyroxene, and bad agreement with garnet below 1375 °C at 3.0 GPa. As displayed in Fig. 6, the comparisons of pMELTS melt compositions with experimental melts at 3.0 GPa show bad agreement, mainly due to SiO_2 (+47 to 230%), Al_2O_3 (−17 to 28%), FeO (−21 to 71%), MgO (−53 to 61%), and CaO (−23.8 to 62%). For Rcrust calculations, bad matches with melt are due to FeO (−33.92 to 60%) and TiO_2 (+56 to 68%), however at lower pressure and above 1365 °C at 3.0 GPa, melt compositions show better matches, ranging from reasonable to good (Table 5 & Fig. 6).

4.2. Uncertainty surrounding experimental results

The full set of thermodynamic modelling results from investigating unintended changes to reported bulk compositions from experimental studies are available in Appendix A. For the purpose of this comparison, particularly in terms of the location of the solidi, the modelling has been extended to 1000 °C, which is beyond the temperature range of the experimental studies.

From the KLB-1 and MM3 results displayed in Fig. 7, it is mainly H_2O addition that causes significant changes in predicted phase assemblages and proportions (Appendix A), where the resultant inhibition or stabilisation of several phases across the P-T range investigated may result in a better or worse match with the experimental assemblages reported. As is expected, H_2O addition also lowers the solidus quite significantly (> 230 °C), which conversely may be shifted by Fe loss to higher temperatures above 2.0 GPa (Appendix A). The shift in the solidi caused by H_2O incorporation results in the increase of the melt fraction of up to 4.7% for KLB-1 and 3.6 wt% for MM3, whereas this increase is less prominent for CO_2 (up to 1.2 wt% increase). Fe loss may result in small variations in olivine, pyroxene, and melt proportions, similarly for clinopyroxene and melt due to CO_2 formation. Compared to experimental data, H_2O and CO_2 addition also decreases the percentage difference of olivine and melt proportions for KLB-1, similarly for MM3 proportions of olivine, clinopyroxene, and melt, and orthopyroxene at higher temperature. This improvement in predicted abundances is much more prominent for H_2O than CO_2. Changes in the compositions of the phases are reported in Appendix A.

5. Discussion

Several general observations can be drawn from the results presented in the previous section. It is important to reiterate that quantitative comparison between experimental and modelled results are extremely unlikely to produce outputs that match perfectly, because of the uncertainties inherent to both sets of findings, as discussed earlier. For upper mantle studies, previously conducted comparative works acknowledge and may briefly discuss these uncertainties (e.g. García-Arias, 2020; Gervais and Trapy, 2021; Ghiorso et al., 2002), but do not attempt quantitative comparison of the effects that well-known causes of experimental uncertainties may have on phase stability and

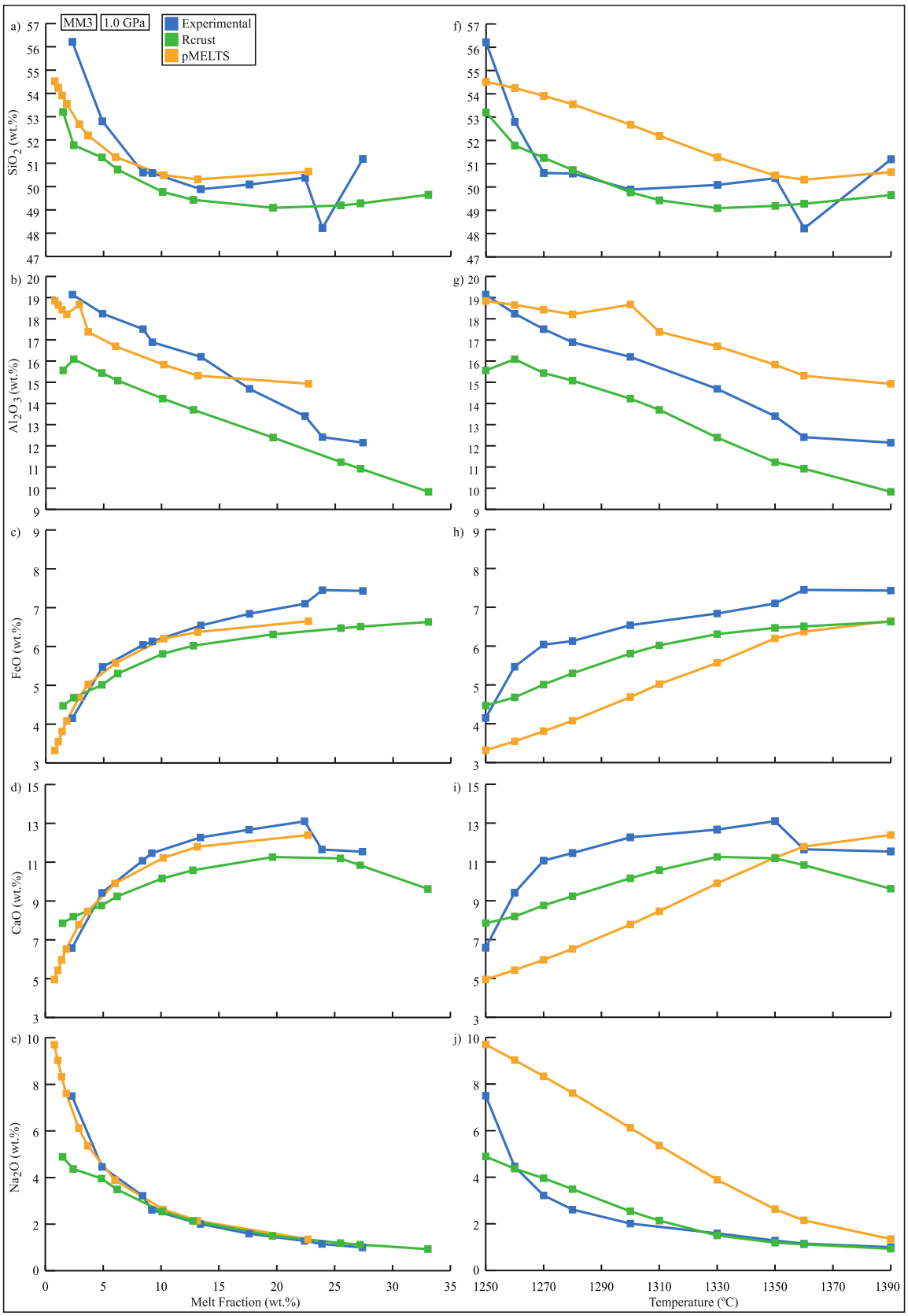

Fig. 4. A comparison of selected components of melt compositions as the melt fraction (a-e) increases and as the temperature (f-j) increases at 1.0 GPa from the experimental study on MM3 of Baker and Stolper (1994) and Hirschmann et al. (1998b), with the calculated values from pMELTS and Rcrust as determined in this study. Both pMELTS and Rcrust show better agreement with experimental values along increasing melt fraction, although Rcrust shows better overall agreement along increasing temperature.

Table 5
Scoring of the modelled assemblages (bulk Q*asm*) and compositions (sum of residuals^2) from pMELTS and Rcrust in comparison with the experimental study on G2 from Pertermann and Hirschmann (2003a, 2003b), where such data was available.

Assemblage: Q*asm*		
	Rcrust	pMELTS
Bulk Q*asm* in 21 experiments	87.65	72.29

Compositions: Sum of residuals^2

	2.0 GPa						2.5 GPa		3.0 GPa	
	1250 °C		1325 °C		1375 °C		1325 °C		1275 °C	
	Rcrust	pMELTS	Rcrust	pMELTS	Rcrust	pMELTS	Rcrust	pMELTS	Rcrust	pMELTS
Cpx	11.16	14.50	17.93	11.70	21.44	12.77	26.93	15.14	10.04	7.10
Gt	13.58	8.28	9.36	4.18	–	–	20.55	7.70	36.74	6.83
Plag	64.93	–	–	–	–	–	–	–	–	–
Melt	63.34	288.20	3.79	69.15	4.43	28.55	16.06	90.46	–	105.05

	3.0 GPa									
	1300 °C		1315 °C		1325 °C		1335 °C		1350 °C	
	Rcrust	pMELTS	Rcrust	pMELTS	Rcrust	pMELTS	Rcrust	pMELTS	Rcrust	pMELTS
Cpx	6.33	17.57	4.58	10.57	5.44	17.84	10.69	18.31	12.43	16.68
Gt	38.72	11.49	36.34	12.36	37.94	12.88	37.33	14.68	32.47	12.87
Melt	–	–	–	305.83	53.06	239.81	43.99	236.43	28.67	211.89

	3.0 GPa									
	1365 °C		1375 °C		1400 °C		1425 °C		1450 °C	
	Rcrust	pMELTS	Rcrust	pMELTS	Rcrust	pMELTS	Rcrust	pMELTS	Rcrust	pMELTS
Cpx	24.49	21.27	26.55	16.52	30.81	17.13	30.63	15.91	34.57	16.91
Gt	29.08	13.93	27.84	14.95	22.73	14.82	14.28	10.38	10.74	10.66
Melt	23.85	184.24	18.47	148.28	19.10	164.44	12.05	140.14	4.43	125.76

	3.0 GPa					
	1450 °C		1475 °C		1500 °C	
	Rcrust	pMELTS	Rcrust	pMELTS	Rcrust	pMELTS
Cpx	34.57	16.91	39.58	21.14	–	19.02
Gt	10.74	10.66	15.08	15.88	–	–
Melt	4.43	125.76	3.85	92.61	1.96	92.56

composition. Using thermodynamic modelling and reasonable estimates of Fe loss and H_2O or CO_2 addition, a potential envelope of uncertainty around the experimental results has been defined (Fig. 7). Changes in fO_2 have not been considered, as the use of graphite liners in all the experimental studies considered here limits the fO_2 to C-CO. The results indicate that a modelled Fe loss of 10% shows little variance in phase proportions and compositions (Fig. 7). The incorporation of a small amount of CO_2 (0.08 wt%) has a similarly small effect on the results, but these effects will be more prominent at higher pressure conditions. The addition of 0.05 wt% H_2O shows a significant shift of the solidus to lower temperatures for both compositions. At any given temperature above the solidus, melt volumes are significantly increased and the abundance of clinopyroxene decreased. These results support two observations: Firstly, although the experimental investigations utilised in this study do not appear to be severely affected by Fe loss and CO_2 formation, unintended H_2O may have been incorporated into the capsules (Fig. 7), which is not considered by Takahashi (1986) to be significant for KLB-1 below 1700 °C, and is noted by Hirschmann et al. (1998b) for MM3 as $\leq$0.4 wt% at higher temperatures only. Secondly, even with the modelled effects of added H_2O and CO_2, or a loss of Fe, differences in the modelling and the experimental melt abundances are still evident. Although this could suggest that the incorporated H_2O may exceed what is modelled and/or reported, this seems unlikely due to the discrepancy of the clinopyroxene abundance when compared to experimental results at the current modelled H_2O weight fraction. Rather, the uncertainties in thermodynamic modelling input data appear to play a larger role in this discrepancy. This has two implications: 1) Experiments considered as 'anhydrous' or 'volatile free' may unintentionally propagate uncertainties into thermodynamic datasets, which are calibrated using experimental phase equilibria and calorimetric data, and in some cases, data of natural mineral partitioning; but (2) does not render all such experimental data as ultimately unreliable for comparisons with modelling at anhydrous conditions, as inherent uncertainties in the thermodynamic input files and calculation strategies cannot be ignored and identified otherwise. Thus, the suggestion of Ghiorso et al. (2002) that a portion of the offset of pMELTS predicted melt fractions of peridotite partial melting are due to 'phantom' volatile incorporation in piston cylinder experiments, which causes an increase in the melt abundance, is reasonable (Appendix A), but this does not surpass the inaccuracies still prevalent in thermodynamic modelling input data or calculation strategies.

Evaluations on the performance of the selected modelling tools to investigate partial melting across a range of temperatures at 1.0 to 3.0 GPa show that the Rcrust bundle displays good to excellent agreement with experimental phase assemblages (Fig. 1; bulk Q*asm* of 78–100%) and proportions (Figs. 2, 3, 5; Appendix A), and predict compositions that mostly agree reasonably with experiments (Tables 3–5; Appendix A), with the most notable discrepancies being spinel, garnet, and melt. The outputs from pMELTS show good to excellent agreement with experimentally determined phase assemblages (bulk Q*asm* of 72–95%) under SCLM conditions, however, greater overall discrepancies can be noted for phase proportions (Figs. 2, 3, 5; Appendix A) as well as for compositions of spinel, melt, and the 3.0 GPa clinopyroxene of KLB-1 (Tables 3–5; Appendix A). These discrepancies are more pronounced for the eclogitic composition (Figs. 5, 6; Table 5).

When considering closed system interactions, the properties of any one phase cannot change without an equal exchange in the accompanying phases, as is evident by the interchanges observed in phase assemblages, compositions, and proportions. Many of the observed discrepancies between experimental studies and thermodynamic calculations can thus be reconciled by considering the effects of predicted phase behaviours on these properties. For the partial melting of eclogite, pMELTS fails to predict the stabilisation of the ilmenite and quartz phases (Fig. 5, Appendix A), with a smooth evolution of melt fraction

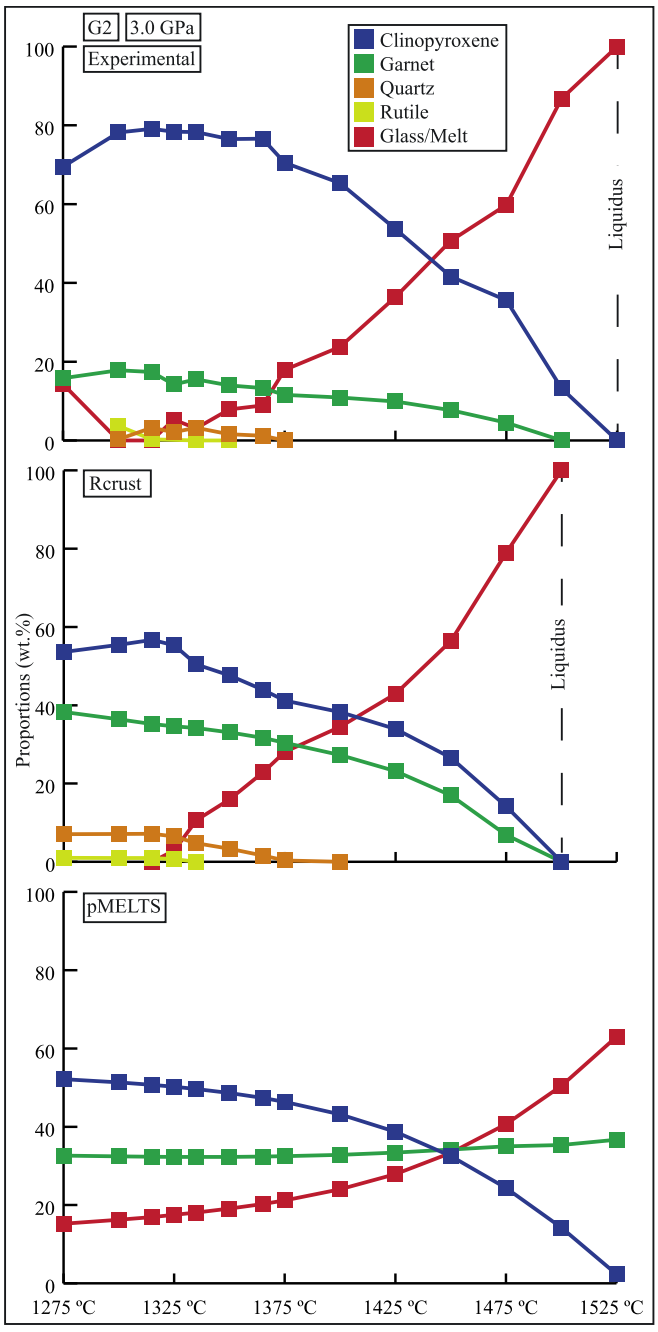

Fig. 5. A comparison of melt (glass), clinopyroxene, garnet, quartz and rutile abundances at 3.0 GPa from the experimental study on G2 of Pertermann and Hirschmann (2003a), with the calculated values from pMELTS and Rcrust as determined by this study. pMELTS predicts the liquidus to be at much higher temperatures than the experiments, whilst there is good agreement between the curve of the melt fraction predicted by Rcrust and the experiments. This is similarly observed for rutile and quartz (although greater phase abundances are predicted by Rcrust), which was not predicted by pMELTS. This lack of quartz results in the pMELTS system not predicting the reactions between garnet and quartz seen in the experiments and in Rcrust, hence the different phase abundance curves observed for pMELTS, and the exhaustion of garnet at higher temperatures. Rcrust predicts the exhaustion of clinopyroxene at lower temperatures than the experiments, whereas pMELTS predicts this at higher temperatures.

increase accompanied by a mirrored decrease in the clinopyroxene as the only phase contributing towards melt formation. For the MM3 comparison of Ghiorso et al. (2002), the authors note the stabilisation of clinopyroxene at the expense of melt, however, the converse is displayed for the eclogite, where clinopyroxene abundances are 17.32 wt% lower, whilst melt is only 0.91 wt% higher. This is likely due to due to the observation of the supersaturation of garnet displayed by pMELTS at higher temperature (Ghiorso et al., 2002). The observed smoothed increase in melt fraction is less obvious for KLB-1 in Fig. 2, but a prominent feature of the comparison is that the system reaches the liquidus at 200 °C lower than the experiments at 1.5 GPa, although melt abundances remain lower than the experiments until ~1550 °C. Distinct inflection points in the temperature-melt fraction trends of pMELTS are visible at 1400 °C and 1550 °C, and because no other inflections occur, the melt fraction increases rapidly and is mirrored by the consumption of olivine (Appendix A). As a result, major overall discrepancies of the melt phase compositions (Tables 3–5) in terms of temperature (as noted in Section 2.4 and by Ghiorso et al., 2002) and eclogitic melt fractions (Figs. 4, 6) are observed at high and low pressures (Table 4). Of note is that pMELTS calculations of olivine and clinopyroxene compositions (sans KLB-1 at 3.0 GPa) show reasonable to good agreement with experiments, fitting slightly better at low pressures for the peridotites (Tables 3, 4) and at higher temperatures at 3.0 GPa for the eclogite (Table 5) than Rcrust predicted compositions. It thus appears that although pMELTS is generally effective at phase assemblage predictions and compositions of specific phases, particularly for peridotite partial melting, the predicted melt fraction has a strong temperature dependence (Figs. 2, 4, 6). This influences the proportions and compositions of several phases, although this is less obvious at lower P-T conditions such as those investigated for MM3. Ultimately, melt compositions predicted by pMELTS for the eclogite may vary noticeably from experimental results because of the overstabilisation of melt relative to clinopyroxene or olivine, which are subsequently exhausted from the system more quickly. Ghiorso et al. (2002) note unsatisfactory results for pMELTS predictions of peridotite partial melting from 3.0 to 7.0 GPa, but as is displayed here, this is also evident for more basaltic compositions from 2.0 to 3.0 GPa.

Overall, Rcrust predicted phase proportions display a comparable increase in melt fraction to that of the experiments (Figs. 2, 3, 5), mostly displaying the sudden drops or increases in the phase proportions as melt volume increases, regardless of phases missing in the assemblage or differences in the predicted initial proportions of phases and their rates of consumption. For example, although the liquidus is displaced to 50 °C higher in Fig. 2 for KLB-1, the increase in melt fraction and subsequent rate of olivine consumption (Appendix A) predicted by Rcrust is comparable with the experimental study. For the eclogite, Rcrust predicts increased garnet and decreased clinopyroxene proportions as compared to the experiments (Fig. 5). Clinopyroxene is consumed more rapidly, and due to its lower proportions, is exhausted at the same temperature as garnet. Conversely, because clinopyroxene has higher proportions in the experimental results, it is exhausted at a higher temperature due to its rate of consumption. Although this difference influences the melt proportion at lower temperatures, the curve of the melt fraction mostly follows that of the experiments and thus produce mostly similar melt compositions, apart from FeO content (Fig. 6). Similar behaviour can be noted in Fig. 3, although melt components show notable variation from experimental results for peridotite partial melting.

It is clear that the discrepancies displayed by pMELTS and Rcrust compared to experimental results are likely as a result of differences in the thermodynamic datasets and formulation of the *a-x* models (particularly the melt *a-x* model), because the calculation strategy of the software are reported as similar (Table 1). The interactions of *a-x* models with the thermodynamic dataset should also be taken into consideration. The input data clearly result in notable variance across P-T-X space, but unfortunately, due to the embedded nature of these input components in the pMELTS software, this cannot be investigated in more

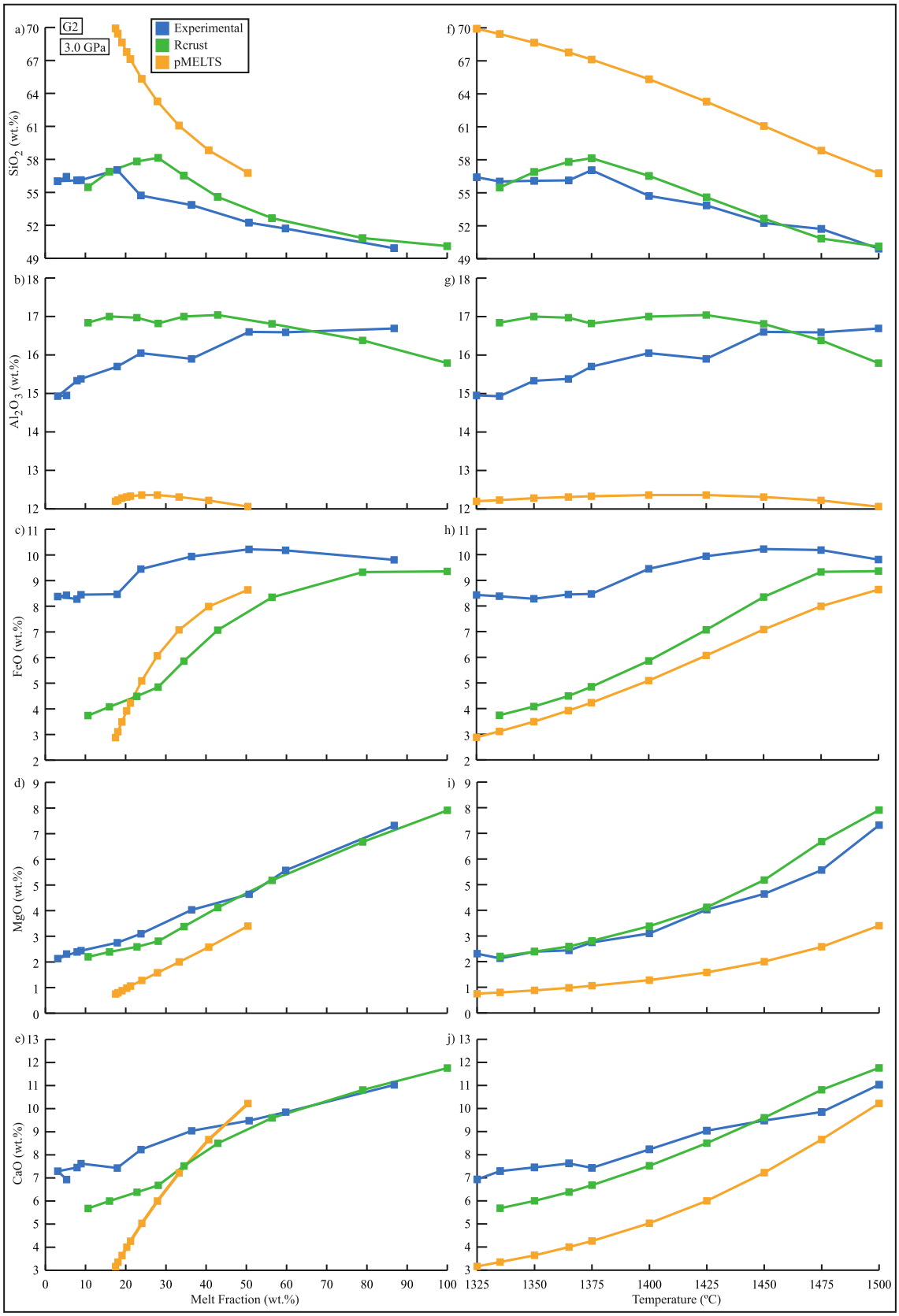

Fig. 6. A comparison of selected components of melt compositions as the melt fraction (a-e) increases and as the temperature (f-j) increases at 3.0 GPa from the experimental study on G2 from Pertermann and Hirschmann (2003a, 2003b) with the calculated values from Rcrust and pMELTS as determined in this study. Rcrust predicted melt compositions range from bad to good in terms of agreement with experimental melt compositions, depending on the component. As discussed in-text, pMELTS indicates significantly lower values for several of the melt phase components, showing bad agreement with experimental melts in terms of melt fraction and temperature.

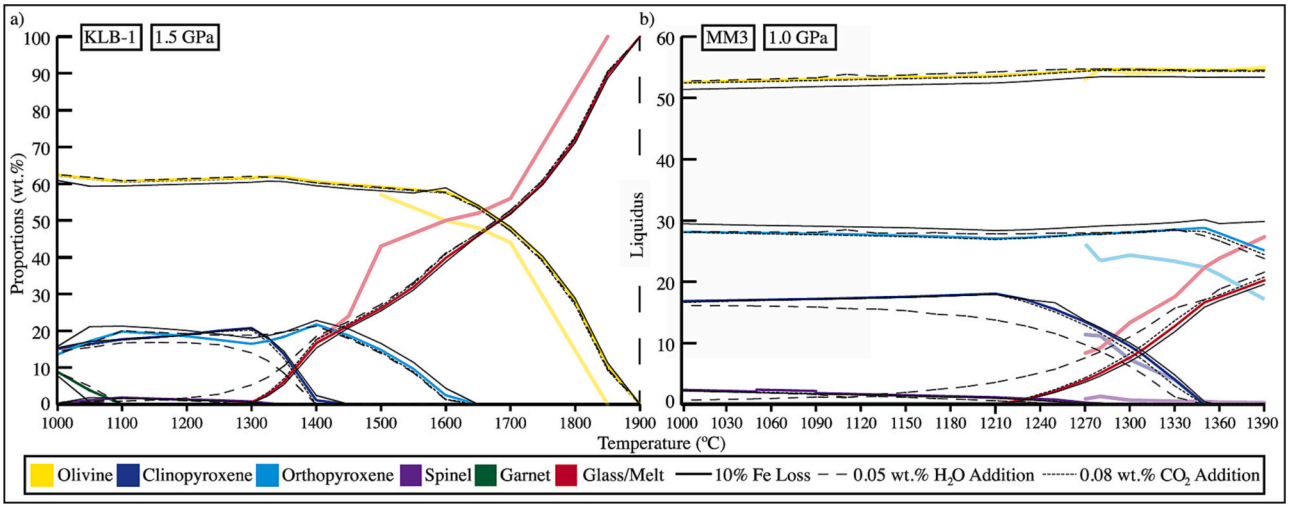

Fig. 7. A comparison of changes in phase abundances with increasing temperature as a result of minor amounts of Fe loss to the capsule, or the incorporation of very small amounts of H_2O or CO_2 in the capsule. Phase proportions reported by the experimental studies are included in faded colouring. a) Adjustment modelling of the 1.5 GPa experiments on KLB-1 of Takahashi (1986) and Takahashi et al. (1993), extended down to 1000 °C. b) Adjustment modelling of the 1.0 GPa experiments on MM3 of Baker and Stolper (1994) and Hirschmann et al. (1998b), extended down to 1000 °C. H_2O addition of 0.05 wt% results in the extensive lowering of the solidus and decrease in clinopyroxene abundance. An increase in the melt fraction can be observed distinctly below 1500 °C for both comparisons.

detail. Similar discrepancies have been noted where software utilise the same thermodynamic dataset and related *a-x* models, which may be a result of two important factors: The requirement of HP*x*-eos families to be formatted for use in Perple_X (and subsequently, Rcrust and others) mean that small oversights or mistakes, or even a delay in the formatting process can easily result in a mismatch in the predicted outcomes. The second factor is the calculation method of the software, where different strategies can cause mismatches due to user-specified parameters inherent to the strategy. For example, failing to identify assemblage tie-lines in THERMOCALC could exclude an entire assemblage field from the pseudosection, or not implementing the appropriate resolution in Perple_X (and Rcrust) would cause a failure to identify phases or even small assemblage fields. Evidently, thermodynamic input data or calculation strategies can have implications on the results produced by thermodynamic modelling when compared to experiments, not without taking into consideration the mismatches that may be as a result of experimental pitfalls, as is discussed earlier.

6. Conclusions

This comparative study supports two primary conclusions. Firstly, when compared with experimental results, the use of phase equilibrium modelling routines is a viable method for analysing the phase assemblages, proportions, and compositions in ultramafic and mafic rock compositions under SCLM P-T conditions. This approach should be seen as complementary to experimental work, with several advantages such as being an extremely rapid form of investigation when compared to experimental studies, allowing greater P-T-X resolution and control over the incorporation of volatiles, as well as their fugacities. Secondly, Rcrust using Gibbs free energy minimisation from Perple_X, the internally consistent dataset of Holland and Powell (2011), and the *a-x* models of clinopyroxene, garnet, orthopyroxene, spinel, and melt (Tomlinson and Holland, 2021), olivine (Holland et al., 2018), feldspar (Holland and Powell, 2003), and ilmenite (White et al., 2000), generally mapped out melt production and compositions reliably at SCLM P-Ts, when compared with the experimental results. The software, *a-x* models and thermodynamic dataset are a good combination for studying petrogenic processes where the melt fraction changes significantly within the P-T-X range of this study, and for compositions that range from ultramafic to mafic. This, in combination with the capability of Rcrust to allow phase extraction and accommodate the resultant bulk compositional change, makes the Rcrust methodology presented here well-suited for the study of partial melting reactions in the upper mantle, including the effects of magma segregation.

Declaration of Competing Interest

The authors declare that they have no known competing financial interests or personal relationships that could have appeared to influence the work reported in this paper.

Acknowledgements

The authors thank M. Garçia-Arias and an anonymous reviewer for their comments and suggestions that aided in the improvement of this manuscript. This work was supported by the South African National Research Foundation (NRF) through the South African Research Chairs Initiative (SARChI) awarded to G. Stevens, and the BuCoMO International Research Project (IRP) by the French Centre for Scientific Research (CNRS) and the NRF.

Appendix A. Supplementary data

Supplementary data to this article can be found online at https://doi.org/10.1016/j.lithos.2023.107111.

References

Asimow, P.D., Ghiorso, M.S., 1998. Algorithmic modifications extending MELTS to calculate subsolidus phase relations. Am. Mineral. 83, 1127–1132.
Asimow, P.D., Dixon, J.E., Langmuir, C.H., 2004. A hydrous melting and fractionation model for mid-ocean ridge basalts: application to the mid-Atlantic ridge near the Azores. Geochem. Geophys. Geosyst. 5, 1.
Baker, M.B., Stolper, E.M., 1994. Determining the composition of high-pressure mantle melts using diamond aggregates. Geochim. Cosmochim. Acta 58, 2811–2827.
Berman, R.G., 1988. Internally-consistent thermodynamic data for minerals in the system Na_2O-K_2O-CaO-MgO-FeO-Fe_2O_3-Al_2O_3-SiO_2-TiO_2-H_2O-CO_2. J. Petrol. 29, 445–522.
Bohrson, W.A., Spera, F.J., Ghiorso, M.S., Brown, G.A., Creamer, J.B., Mayfield, A., 2014. Thermodynamic model for energy-constrained open-system evolution of crustal magma bodies undergoing simultaneous recharge, assimilation and crystallization: the Magma chamber simulator. J. Petrol. 55, 1685–1717.
Brugier, Y.-A., Alletti, M., Pichavant, M., 2015. Fe pre-enrichment: a new method to counteract iron loss in experiments on basaltic melts. Am. Mineral. 100, 2106–2111.
Cawthorn, R.G., Ford, C.E., Biggar, G.M., Bravo, M.S., Clarke, D.B., 1973. Determination of the liquid composition in experimental samples: discrepancies between microprobe analysis and other methods. Earth Planet. Sci. Lett. 21, l–5.

Connolly, J.A.D., 2005. Computation of phase equilibria by linear programming: a tool for geodynamic modeling and its application to subduction zone decarbonation. Earth Planet. Sci. Lett. 236, 524–541.
Connolly, J.A.D., 2007. Perple_X Comparisons [Online]. Available: https://www.perplex.ethz.ch/perplex_thermocalc_comparison.html [2022, November 4].
Connolly, J.A.D., 2009. The geodynamic equation of state: what and how. Geochem. Geophys. Geosyst. 10, 10.
Connolly, J.A.D., 2021. Index of/Perplex/Examples [Online]. Available: https://www.perplex.ethz.ch/perplex/examples/ [2022, November 10].
Connolly, J.A.D., 2022. Perple_X Updates [Online]. Available: https://hpxeosandthermocalc.org/2020/10/31/high-ca-opx-again/ [2021, May 13].
Connolly, J.A.D., Kerrick, D.M., 1987. An algorithm and computer program for calculating composition phase diagrams. CALPHAD 11, 1–55.
Connolly, J.A.D., Petrini, K., 2002. An automated strategy for calculation of phase diagram sections and retrieval of rock properties as a function of physical conditions. J. Metamorph. Geol. 20, 697–708.
de Capitani, C., Brown, T.H., 1987. The computation of chemical equilibrium in complex systems containing non-ideal solutions. Geochim. Cosmochim. Acta 51, 2639–2652.
de Capitani, C., Petrakakis, K., 2010. The computation of equilibrium assemblage diagrams with Theriak/Domino software. Am. Mineral. 95, 1006–1016.
Duesterhoeft, E., de Capitani, C., 2013. Theriak_D: an add-on to implement equilibrium computations in geodynamic models. Geochem. Geophys. Geosyst. 14, 4962–4967.
Falloon, T.J., Green, D.H., Hatton, C.J., Harris, K.L., 1988. Anhydrous partial melting of a fertile and depleted peridotite from 2 to 30 kb and application to basalt petrogenesis. J. Petrol. 29, 1257–1282.
Falloon, T.J., Green, D.H., O'Neill, H.S.C., Ballhaus, C.G., 1996. Quest for low degree partial melts. Nature 381, 285.
Falloon, T.J., Green, D.H., Danyushevsky, L.V., Faul, U.H., 1999. Peridotite melting at 1.0 and 1.5 GPa: an experimental evaluation of techniques using diamond aggregates and mineral mixes for determination of near-solidus melts. J. Petrol. 40, 1343–1375.
Forshaw, J.B., Waters, D.J., Pattinson, D.R.M., Palin, R.M., Gopon, P., 2019. A comparison of observed and thermodynamically predicted phase equilibria and mineral compositions in mafic granulites. J. Metamorph. Geol. 37, 15–179.
García-Arias, M., 2020. Consistency of the activity–composition models of Holland, Green, and Powell (2018) with experiments on natural and synthetic compositions: a comparative study. J. Metamorph. Geol. 38, 993–1010.
Gervais, F., Trapy, P.-H., 2021. Testing solution models for phase equilibrium (forward) modeling of partial melting experiments. Contrib. Mineral. Petrol. 167, 4.
Ghiorso, M.S., Gualda, G.A.R., 2015. An H_2O–CO_2 mixed fluid saturation model compatible with rhyolite-MELTS. Contrib. Mineral. Petrol. 169, 53.
Ghiorso, M.S., Sack, R.O., 1995. Chemical mass transfer in magmatic processes, IV. A revised and internally consistent thermodynamic model for the interpolation and extrapolation of liquid-solid equilibria in magmatic systems at elevated temperatures and pressures. Contrib. Mineral. Petrol. 119, 197–212.
Ghiorso, M.S., Hirschmann, M.M., Reiners, P.W., Kress, V.C.I.I.I., 2002. The pMELTS: a revision of MELTS for improved calculation of phase relations and major element partitioning related to partial melting of the mantle to 3 GPa. Geochem. Geophys. Geosyst. 3, 1–36.
Green, E.C.R., 2020. High-Ca opx again [Online]. Available: https://hpxeosandthermocalc.org/2020/10/31/high-ca-opx-again/ [2021, May 13].
Green, E.C.R., 2022. The HPx-eos and THERMOCALC [Online]. Available: https://hpxeosandthermocalc.org/the-hpx-eos/the-hpx-eos-families/igneous-set/ [2022, Feb 8].
Green, E.C.R., White, R.W., Diener, J.F.A., Powell, R., Holland, T.J.B., Palin, R.M., 2016. Activity-composition relations for the calculation of partial melting equilibria in metabasic rocks. J. Metamorph. Geol. 34, 845–869.
Grove, T.L., 1981. Use of FePt alloys to eliminate the iron loss problem in 1 atmosphere gas mixing experiments: theoretical and practical considerations. Contrib. Mineral. Petrol. 78, 298–304.
Gualda, G.A.R., Ghiorso, M.S., Lemons, R.V., Carley, T.L., 2012. Rhyolite-MELTS: a modified calibration of MELTS optimized for silica-rich, fluid-bearing magmatic systems. J. Petrol. 53, 875–890.
Heinrich, C.A., Connolly, J.A.D., 2022. Physical transport of magmatic sulfides promotes copper enrichment in hydrothermal ore fluids. Geology 50, 1101–1105.
Hernández-Uribe, D., Spera, F.J., Bohrson, W.A., Heinonen, J.S., 2022. A comparative study of two-phase equilibria modeling tools: MORB equilibrium states at variable pressure and H_2O concentrations. Am. Mineral. 107, 1789–1806.
Hirschmann, M.M., Ghiorso, M.S., Wasylenki, L.E., Asimow, P.D., Stolper, E.M., 1998a. Calculation of peridotite partial melting from thermodynamic models of minerals and melts. I. Review of methods and comparison with experiments. J. Petrol. 39, 1091–1115.
Hirschmann, M.M., Baker, M.B., Stolper, E.M., 1998b. The effect of alkalis on the silica content of mantle-derived melts. Geochim. Cosmochim. Acta 62, 883–902.
Holland, T.J.B., Powell, R., 1985. An internally consistent thermodynamic dataset with uncertainties and correlations: 2. Data and results. J. Metamorph. Geol. 3, 343–370.
Holland, T.J.B., Powell, R., 1990. An enlarged and updated internally consistent thermodynamic dataset with uncertainties and correlations: the system Na_2O-K_2O-CaO-MgO-MnO-FeO-Fe_2O_3-Al_2O_3-SiO_2-TiO_2-C-H_2-O_2. J. Metamorph. Geol. 8, 89–124.
Holland, T.J.B., Powell, R., 1996a. Thermodynamics of order–disorder in minerals 1: symmetric formalism applied to minerals of fixed composition. Am. Mineral. 81, 1413–1424.
Holland, T.J.B., Powell, R., 1996b. Thermodynamics of order–disorder in minerals 2: symmetric formalism applied to solid solutions. Am. Mineral. 81, 1425–1437.
Holland, T.J.B., Powell, R., 1998. An internally consistent thermodynamic data set for phases of petrological interest. J. Metamorph. Geol. 16, 309–343.
Holland, T.J.B., Powell, R., 2001. Calculation of phase relations involving haplogranitic melts using an internally consistent thermodynamic dataset. J. Petrol. 42, 673–683.
Holland, T.J.B., Powell, R., 2003. Activity-composition relations for phases in petrological calculations: an asymmetric multicomponent formulation. Contrib. Mineral. Petrol. 145, 492–501.
Holland, T.J.B., Powell, R., 2011. An improved and extended internally consistent thermodynamic dataset for phases of petrological interest, involving a new equation of state for solids. J. Metamorph. Geol. 29, 333–383.
Holland, T.J.B., Green, E.C.R., Powell, R., 2018. Melting of peridotites through to granites: a simple thermodynamic model in the system KNCFMASHTOCr. J. Petrol. 59, 881–900.
Horváth, P., 2007. P-T pseudosections in KFMASH, KMnFMASH, NCKFMASH and NCKMnFMASH systems: a case study from garnet-staurolite mica schist from the Alpine metamorphic basement of the Pannonian Basin (Hungary). Geol. Carpath. 58, 107–119.
Humphreys, M.C.S., Kearns, S.L., Blundy, J.D., 2006. SIMS investigation of electron-beam damage to hydrous, rhyolitic glasses: implications for melt inclusion analysis. Am. Mineral. 91, 667–679.
Ito, K., Kennedy, G.C., 1973. The composition of liquids formed by partial melting of eclogites at high temperatures and pressures. J. Geol. 82, 383–392.
Jennings, E.S., Holland, T.J.B., 2015. A simple thermodynamic model for melting of peridotite in the system NCFMASOCr. J. Petrol. 56, 869–892.
Kushiro, I., 2001. Partial melting experiments on peridotite and origin of mid-ocean ridge basalt. Annu. Rev. Earth Planet. Sci. 29, 71–107.
Lanari, P., Duesterhoeft, E., 2019. Modeling metamorphic rocks using equilibrium thermodynamics and internally consistent databases: past achievements, problems and perspectives. J. Petrol. 60, 19–56.
Mayne, M., Moyen, J.-F., Stevens, G., Kaislaniemi, L., 2016. Rcrust: a tool for calculating path-dependent open system processes and application to melt loss. J. Metamorph. Petrol. 34, 663–682.
Mayne, M., Stevens, G., Moyen, J.-F., Johnson, T., 2019. Performing process-oriented investigations involving mass transfer using Rcrust: a new phase equilibrium modelling tool. In: Janoušek, V., Bonin, B., Collins, W.J., Farina, F., Bowden, P. (Eds.), Post-Archean Granitic Rocks: Petrogenetic Processes and Tectonic Environments, Geological Society of London Special Publications 491, Bath, pp. 209–221.
Médard, E., McCammon, C.A., Barr, J.A., Grove, T.L., 2008. Oxygen fugacity, temperature reproducibility, and H_2O contents of nominally anhydrous piston-cylinder experiments using graphite capsules. Am. Mineral. 93, 1838–1844.
Merrill, R.B., Wyllie, P.J., 1973. Absorption of iron by platinum capsules in high pressure rock melting experiments. Am. Mineral. 58, 16–20.
Morgan, G.B.I.V., London, D., 1996. Optimizing the electron microprobe analysis of hydrous alkali aluminosilicate glasses. Am. Mineral. 81, 1176–1185.
Pertermann, M., Hirschmann, M.M., 2003a. Partial melting experiments on a MORB-like pyroxenite between 2 and 3 GPa: constraints on the presence of pyroxenite in basalt source regions from solidus location and melting rate. J. Geophys. Res. Solid Earth 108, 2125.
Pertermann, M., Hirschmann, M.M., 2003b. Anhydrous partial melting experiments on MORB-like eclogite: phase relations, phase compositions and mineral–melt partitioning of major elements at 2-3 GPa. J. Petrol. 44, 2173–2201.
Powell, R., 1985. Geothermometry and geobarometry: a discussion. J. Geol. Soc. 142, 29–38.
Powell, R., Holland, T.J.B., 1988. An internally consistent dataset with uncertainties and correlations: 3. Applications to geobarometry, worked examples and a computer program. J. Metamorph. Petrol. 6, 173–204.
Powell, R., Holland, T.J.B., 1990. Calculated mineral equilibria in the pelite system. KFMASH (K_2O–FeO–MgO–Al_2O_3–SiO_2–H_2O). Am. Mineral. 75, 367–380.
Powell, R., Holland, T.J.B., 1993. On the formulation of simple mixing models for complex phases. Am. Mineral. 78, 1174–1180.
Powell, R., Holland, T.J.B., Worley, B., 1998. Calculating phase diagrams involving solid solutions via non-linear equations, with examples using THERMOCALC. J. Metamorph. Geol. 16, 577–588.
Riel, N., Kaus, B.J.P., Green, E.C.R., Berlie, N., 2022. MAGEMin, an efficient gibbs energy minimizer: application to igneous systems. Geochem. Geophys. Geosyst. 23 e2022GC010427.
Sack, R.O., Ghiorso, M.S., 1994. Thermodynamics of multi-component pyroxenes. 3. Calibration of $Fe^{2+}(Mg)_{-1}$, $TiAl_2(MgSi_2)_{-1}$, $TiFe^{3+}_2(MgSi_2)_{-1}$, $AlFe^{3+}(MgSi)_{-1}$, NaAl$(CaMg)_{-1}$, $Al_2(MgSi)_{-1}$ and ca$(Mg)_{-1}$ exchange-reactions between pyroxenes and silicate melts. Contrib. Mineral. Petrol. 118, 271–296.
Schilling, F., Wunder, B., 2004. Temperature distribution in piston-cylinder assemblies: numerical simulations and laboratory experiments. Eur. J. Mineral. 16, 7–14.
Stevens, G., Clemens, J.D., Droop, T.R., 1997. Melt production during granulite-facies anatexis: experimental data from "primitive" metasedimentary protoliths. Contrib. Mineral. Petrol. 128, 352–370.
Takahashi, E., 1986. Melting of a dry peridotite KLB-1 up to 14 GPa: implications on the origin of peridotitic upper mantle. J. Geophys. Res. 91, 9367–9382.
Takahashi, E., Shimazaki, T., Tsuzaki, Y., Yoshida, H., 1993. Melting study of a peridotite KLB–1 to 6.5 GPa, and the origin of basaltic magmas. Philos. Trans. Phys. Sci. Eng. 342, 105–120.
Tomlinson, E.L., Holland, T.J.B., 2021. A thermodynamic model for the subsolidus evolution and melting of peridotite. J. Petrol. 62 egab012.
Tropper, P., Hauzenberger, C., 2015. How well do pseudosection calculations reproduce simple experiments using natural rocks: an example from high-P high-T granulites of the Bohemian Massif. Aust. J. Earth Sci. 108, 123–138.

Varshneya, A.K., Cooper, A.R., Cable, M., 1966. Changes in composition during electron microprobe analysis of K_2O-SrO-SiO_2 glass. J. Appl. Phys. 37, 2199–2202.
Wang, J., Xiaolin, X., Zhang, L., Takahashi, E., 2020. Element loss to platinum capsules in high-temperature-pressure experiments. Am. Mineral. 105, 1593–1597.
Wasylenki, L.E., Baker, M.B., Hirschmann, H.H., Stolper, E.M., 1996. The effect of source depletion on equilibrium mantle melting. In: EOS Transactions, American Geophysical Union, 77, p. F847.
Wasylenki, L.E., Baker, M.B., Kent, A.J.R., Stolper, E.M., 2003. Near-solidus melting of the shallow upper mantle: partial melting experiments on depleted peridotite. J. Petrol. 44, 1163–1191.
White, R.W., Powell, R., Holland, T.J.B., Worley, B.A., 2000. The effect of TiO_2 and Fe_2O_3 on metapelitic assemblages at greenschist and amphibolite facies conditions: mineral equilibria calculations in the system K_2O–FeO–MgO–Al_2O_3–SiO_2–H_2O–TiO_2–Fe_2O_3. J. Metamorph. Geol. 18, 497–512.
White, R.W., Powell, R., Holland, T.J.B., 2007. Progress relating to calculation of partial melting equilibria for metapelites. J. Metamorph. Petrol. 25, 511–527.
White, R.W., Stevens, G., Johnson, T.E., 2011. Is the crucible reproducible? Reconciling melting experiments with thermodynamic calculations. Elements 7, 241–246.
White, R.W., Powell, R., Holland, T.J.B., Johnson, T.E., Green, E.C.R., 2014. New mineral activity-composition relations for thermodynamic calculations in metapelitic systems. J. Metamorph. Geol. 32, 261–286.
Worley, B.A., Powell, R., 2002. High-precision relative thermobarometry: theory and a worked example. J. Metamorph. Geol. 18, 91–101.
Xiang, H., Connolly, J.A., 2022. GeoPS: an interactive visual computing tool for thermodynamic modelling of phase equilibria. J. Metamorph. Geol. 40, 243–255.